A system of conservation laws with discontinuous flux modelling flotation with sedimentation

Raimund Bürger

Cl²MA and Departamento de Ingeniería Matemática
Universidad de Concepción, Casilla 160-C, Concepción, Chile
rburger@ing-mat.udec.cl

Stefan Diehl

Centre for Mathematical Sciences, Lund University
P.O. Box 118, S-221 00 Lund, Sweden
stefan.diehl@math.lth.se

María del Carmen Martí

Departament de Matemàtiques, Universitat de València
Avda. Vicent Andrés Estellés s/n, Burjasssot, València, Spain
Maria.C.Marti@uv.es

Received (Day Month Year)
Revised (Day Month Year)
Communicated by (xxxxxxxxxx)

The continuous unit operation of flotation is extensively used in mineral processing, wastewater treatment, and other applications for selectively separating hydrophobic particles (or droplets) from hydrophilic ones, where both are suspended in a viscous fluid. Within a flotation column, the hydrophobic particles are attached to gas bubbles that are injected and float as aggregates forming a foam or froth at the top that is skimmed. The hydrophilic particles sediment and are discharged at the bottom. The hydrodynamics of a flotation column is described in simplified form by studying three phases, namely the fluid, the aggregates, and solid particles, in one space dimension. The relative movements between the phases are given by constitutive drift flux functions. The resulting model is a system of two scalar conservation laws with a multiply discontinuous flux for the aggregates and solids volume fractions as functions of height and time. The model is of triangular nature since one equation can be solved independently of the other. Based on the theory of conservation laws with discontinuous flux, steady-state solutions that satisfy all jump and entropy conditions are constructed. For the existence of the industrially relevant steady states, conditions on feed flows and concentrations are established and mapped as "operating charts". A numerical method that exploits the triangular structure, is formulated on a pair of staggered grids, and is employed for the simulation of the fill-up and transitions between steady states of the flotation column.

Keywords: Kinematic flow models, flotation, sedimentation, conservation law, discontinuous flux, non-strictly hyperbolic triangular system.

AMS Subject Classification: Primary: 35L65, 35R05; Secondary: 76T10

1. Introduction

1.1. *Scope*

The flotation process, also known as froth flotation, is a process for selectively separating hydrophobic materials (that are repelled by water) from hydrophilic (that would be attracted to water), where both are supposed to be present as a disperse phase suspended in a viscous fluid. A typical application is the recovery of valuable minerals, such as copper- and lead-bearing minerals, from low-grade ores. This physico-chemical separation process functions roughly as follows: gas is introduced close to the bottom of a column (see Fig. 1), and the bubbles generated rise upward throughout the pulp that contains the solid particles, which can be divided in two main groups. The hydrophobic particles (minerals or ores that should be recovered) attach to the bubbles that float to the top of the column, forming foam or froth carrying the valuable material (the concentrate in mining) that is removed usually through a launder. On the other hand, the hydrophilic particles, also known as slimes or gangue, do not attach to bubbles, but remain and settle to the bottom of the vessel, unless they are trapped in the bulk upflow. Close to the top, additional wash water can be injected to assist with the rejection of entrained impurities[46] and to increase the froth stability and improve recovery.[27,38]

Partly based on Refs. 16, 28, 43, we presented in Ref. 8 a one-dimensional two-phase model describing only the movement of gas bubbles and fluid. The flotation column in Ref. 8 has a separate gas inlet near the bottom, which is commonly used in mineral processing. The hydrophobic particles then attach to the gas bubbles inside the column. Other devices have a common feed inlet for both slurry and gas bubbles, so that the aggregation process, the attachment of hydrophobic particles to bubbles, mostly occurs in the inlet pipe. Here, we model such a column (see Fig. 1) and assume that the bubbles are fully loaded with hydrophobic particles as the mixture enters the column, so that no aggregation occurs inside the column.

The two-phase model in Ref. 8 is a nonlinear scalar conservation law with a multiply discontinuous flux function because of the feed sources of gas, feed slurry, and wash water, and the lower and upper outlets of tailings and concentrate, respectively. It is the purpose of this contribution to extend that formulation and advance a new spatially one-dimensional three-phase model that also includes the settling of solid particles within the flotation column. The three-phase flow of solids, gas (bubbles or aggregates) and fluid is modelled in one dimension. The governing partial differential equations (PDEs) can be written as the system

$$\frac{\partial}{\partial t}\left(A(z)\begin{pmatrix}\phi\\(1-\phi)\varphi\end{pmatrix}\right)+\frac{\partial}{\partial z}\left(A(z)\begin{pmatrix}J(\phi,z,t)\\-F(\varphi,\phi,z,t)\end{pmatrix}\right)=Q_{\mathrm{F}}(t)\begin{pmatrix}\phi_{\mathrm{F}}(t)\\\phi_{\mathrm{s,F}}(t)\end{pmatrix}\delta_{z_{\mathrm{F}}}, \tag{1.1}$$

where the independent variables are time $t>0$ and height $z\in\mathbb{R}$. The unknowns are the volume fraction of bubbles $\phi\in[0,1)$ and $\varphi=\phi_{\mathrm{s}}/(1-\phi)$, where $\phi_{\mathrm{s}}\in[0,1)$ is the volume fraction of solids. Both unknowns are functions of height z and time t. The

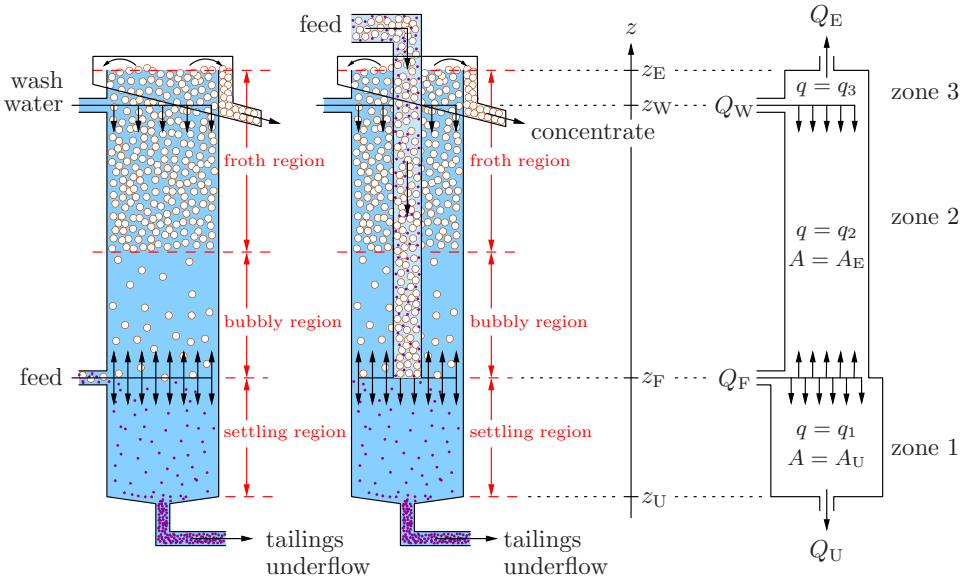

Fig. 1. Left: Schematic of a flotation column with constant cross-sectional area,[27] including heights of feed inlets z_F and z_W, the underflow level z_U and the effluent level z_E. Middle: A schematic of a column with feed inlet downcomer; cf. the Reflux Flotation Cell by Dickinson and Galvin.[16,28] Right: Corresponding conceptual model of the flotation column indicating the volumetric flows of the feed Q_F, wash water Q_W, underflow Q_U and effluent Q_E, and the spatially piecewise constant bulk velocity $q = q(z,t)$. The one-dimensional model with three zones inside the column are complemented with underflow and effluent zones in $z < z_U$ and $z > z_E$, respectively.

flux functions $J(\phi, z, t)$ and $F(\varphi, \phi, z, t)$ contain nonlinear constitutive functions of ϕ and φ that describe the rise of bubbles and settling of solids. The fluxes J and F are discontinuous in z at several positions associated with singular feed sources, the underflow and the effluent, and depend on t via the possibly time varying in- and outflows. The possibly varying cross-sectional area is denoted by $A(z)$. The right-hand side of the equation contains the Dirac measure $\delta_{z_F}(\cdot) := \delta(\cdot - z_F)$ and given positive source functions.

The novelty of this contribution, besides the derivation of (1.1) that will be made explicit in later parts of the paper, is firstly, an analysis of possible steady states, that is, stationary solutions, which have layers of different concentrations of bubbles (foam) and particles separated by discontinuities in concentration. Since the system (1.1) is triangular, our approach is to solve each equation locally as a scalar conservation law with discontinuous flux and use the entropy condition of Ref. 17, which gives the vanishing viscosity entropy solution.[1] The resulting steady states represent the stationary modes of operation of a flotation column without changing control parameters. Roughly speaking, our main result is a characterization of steady states of (1.1), along with restrictions on feed flows and other parameters

for their existence. Here we single out those steady states that are relevant for operation in real applications and visualize in so-called *operating charts* the necessary constraints for the control of the volumetric flows.

Secondly, we advance a numerical difference scheme for (1.1) that treats the equations consecutively, and where the basic idea is to place discontinuities of coefficients inside cells so that the usual Godunov method can be applied and the scheme, which is based on a pair of staggered grids (one for each unknown), becomes simple. The scheme satisfies an invariant region principle (producing approximate volume fractions between zero and one). Two examples show its use for simulating flotation column operations, such as transitions between steady states.

1.2. *Related work*

The two-phase flow of rising bubbles in a liquid has often been modelled with the drift-flux theory by Wallis;[47] see, e.g., Refs 6, 15, 16, 28, 29, 43, 46. The theory considers the relationships between the nonlinear flux of bubbles relative to the fluid (denoted here the batch drift flux) and the applied bulk flows that arise due to the inlets and outlets of the column. The drift-flux theory means a rigorous way of investigating the hydrodynamics in one dimension; however, it is applicable under steady-state conditions only. In this way Stevenson et al.[42] analysed steady-state conditions for settling gangue in foam.

It is well known that the batch drift flux is a particular nonlinear function of the local volume fraction of bubbles. This form has been verified experimentally. The function is unimodal with one inflection point to the right of the maximum. The same qualitative shape has the well-known nonlinear batch settling flux of small particles that settle in a fluid.[35] As pointed out by Stevenson et al.,[43] the flotation column shown in Figure 1 with one inlet of gas and fluid (or suspension) works in principle as an inverted clarifier-thickener used for continuous sedimentation. The corresponding theory for sedimentation for particles in a liquid started with Kynch[35] and is often denoted the solids-flux theory.[19,20,23,24,36]

PDE models for this type of processes have inherent difficulties with non-uniqueness for two reasons. One is the nonlinear batch-flux functions: for a given flux, there may be more than one volume fraction possible. The other reason is caused by the fact that the inlet flux should be split into two. Nature chooses a single solution; however, the non-uniqueness is a known problem for PDE models of sedimentation that are derived from fundamental principles, like the conservation of mass and linear momentum.[3,14] Conservation laws with discontinuous flux are here a key ingredient for which specific entropy conditions[1,5,17,21,30] and numerical schemes[13] have been developed to get the physically correct solutions. In particular, Karlsen and Towers[33] proved that the scalar version of the scheme introduced herein produces the vanishing viscosity entropy solutions. The theoretical results have motivated further analysis of the continuous sedimentation process with applications to control in mineral processing and wastewater treatment.[10,11,18,19,22]

Related areas of application of similar PDE models, where flux discontinuities also appear, include vehicular traffic and crowd dynamics; see Refs. 4, 12, 45 and references therein. Conservation laws with discontinuous flux also appear in models of supply chains or factories with finite work in progress buffer,[2] and geologic carbon dioxide migration and storage.[7]

To the authors' knowledge, the process of flotation (mathematically analogous to that of continuous sedimentation) has not yet been described by PDEs that would be based on these theories developed since the 1990s. Bascur[3] noticed that his two-phase framework could be used for both solid-liquid and gas-liquid separation processes. Several modelling aspects of the processes in a flotation column are given by Cruz,[15] who also reviewed earlier works. Tian et al.[44] set up a hyperbolic system that includes the attachment process; however, they assume that the flux functions are linear. While the vast majority of references to flotation processes are related to mineral processing, we mention that flotation processes are also used for removing other small particles, oil droplets, printing ink and organic matter in diverse processes such as wastewater treatment.[25,26,40,41]

1.3. *Outline of the paper*

The remainder if this work is organized as follows. In Section 2 we introduce the mathematical model. The flotation column is modelled in one spatial dimension, i.e. we assume that all variables depend only on height z and time t. The corresponding volumetric flows and the cross-sectional area are specified in Section 2.1. The fluid, solid (particle), and aggregate (bubble) phases are described in Section 2.2, and the corresponding balance equations are introduced in Section 2.3. To convert these equations into a solvable model, we utilize in Section 2.4 well-known constitutive assumptions for the flux of bubbles rising in a flotation column relative to the suspension (drift-flux theory) and the settling of particles in a liquid (solids-flux theory). In particular, we arrive at algebraic expressions for the total flux functions J and F arising in in (1.1). These functions involve material specific constitutive functions that are introduced in Section 2.5. The properties of the resulting zone flux functions (for the aggregates and the particles), corresponding to the algebraic form of J and F in each zone, are discussed in Section 2.6. In Section 2.7 we comment on properties of (1.1) related to hyperbolicity and entropy solutions arising from the assumptions introduced so far. Section 2 concludes with Section 2.8 that outlines construction of stationary (steady-state) solutions of a conservation law with discontinuous flux, in particular the entropy conditions.

Sections 3, 4 and 5 describe the construction of steady-state solutions of (1.1). Section 3 deals with with steady states for the aggregate phase, in part following Ref. 8 where we classified all steady-solutions for a model that only takes into account gas bubbles and fluid, and where the flotation column has separate inlets of gas and feed slurry. The steady states for ϕ are made possible through the jump conditions (called *couplings* herein) across z_{U} and z_{E}, z_{F}, and z_{W} are analysed in

Sections 3.1, 3.2 and 3.3, respectively. The information is summarized in Section 3.4. We denote by a *desired* steady-state solution a steady-state solution for which no aggregates leave through the bottom and there is a layer of froth at the top of the column. (This is desired for stationary continuous operation in most applications.) Such steady states (for ϕ) are singled out in Section 3.5. The result are four qualitatively different desired steady states for ϕ. In Section 4, we identify the corresponding steady states for the solid phase. The couplings across z_{U} and z_{E}, z_{W}, and z_{F} are analysed in Sections 4.1, 4.2 and 4.3, respectively. The steady states for solids are summarized in Section 4.4. In Section 5 we analyse the existence of desired steady states with and without wash water. The corresponding desired steady-state solutions for the solid phase are constructed in Sections 5.2, 5.3 and 5.4.

The necessary conditions for the different steady states presented in Sections 3, 4 and 5 are nonlinear inequalities and equalities involving the volumetric flows Q_{U}, Q_{F}, Q_{W}, and the incoming volume fractions of aggregates ϕ_{F} and solids $\phi_{\mathrm{s,F}}$. In Section 6, we assume that the feed volume fractions ϕ_{F} and $\phi_{\mathrm{s,F}}$ are given and present restrictions on the control variables Q_{F}, Q_{U} and Q_{W} for each qualitatively possible desired steady state. Then in many cases these inequalities can be visualized as two-dimensional regions in the $(Q_{\mathrm{U}}, Q_{\mathrm{F}})$-plane which we call *operating charts*; these plots provide information on how these parameters can be chosen to attain a determined steady state. These charts are generated in Sections 6.1 to 6.10 for ten different combinations of desired steady states of the aggregate and solids phases.

Finally, we introduce in Section 7 a numerical method to solve (1.1), and thereby to simulate the flotation process. The method is introduced in Section 7.1, which also includes a statement of the invariant region property of the method (numerical values of concentrations assume physically revelant values between zero and one). Two numerical examples of fillup of a flotation columns and transitions between steady states are presented in Section 7.2. Conclusions are collected in Section 8.

2. Mathematical model

2.1. *Volumetric flows and cross-sectional area*

The unit is fed with wash water at level $z = z_{\mathrm{W}}$ and a mixture of aggregates and feed slurry at $z = z_{\mathrm{F}}$; see Fig. 1, where $z_{\mathrm{U}} < z_{\mathrm{F}} < z_{\mathrm{W}} < z_{\mathrm{E}}$ divide the real line into the zones inside the column and the underflow and effluent zones. The corresponding volumetric feed flows of wash water, $Q_{\mathrm{W}} \geq 0$, and of feed slurry, $Q_{\mathrm{F}} > 0$, are given functions of time, as is the volumetric underflow rate $Q_{\mathrm{U}} \geq 0$. The resulting effluent volumetric overflow $Q_{\mathrm{E}} = Q_{\mathrm{W}} + Q_{\mathrm{F}} - Q_{\mathrm{U}}$ is assumed to be nonnegative so that the mixture is conserved and the vessel is always completely filled with mixture.

To model a feed inlet pipe located in the upper part and centre of a cylindrical column, the cross-sectional area is assumed to have a discontinuity at the feed inlet:

$$A(z) = \begin{cases} A_{\mathrm{E}} & \text{for } z \geq z_{\mathrm{F}}, \\ A_{\mathrm{U}} & \text{for } z < z_{\mathrm{F}}, \end{cases} \quad \text{where } A_{\mathrm{E}} \leq A_{\mathrm{U}}. \tag{2.1}$$

In our examples we will use the measures corresponding to the flotation column that is part of the Reflux Flotation Cell used by Dickinson and Galvin.[16,28] The flotation column is 1 m high with a cross-sectional area of $A_{\mathrm{U}} = 83.65\,\mathrm{cm}^2$. Feed slurry and gas bubbles are pumped through a downcomer of external diameter 3.81 cm, which forms an annulus around a 2.54 cm-diameter tube that incorporates a porous sparger for bubble creation. Hence, the effective horizontal cross-sectional area above the feed inlet is $A_{\mathrm{E}} = 72.25\,\mathrm{cm}^2$. The outlet of the downcomer is positioned 66.7 cm below the top of the vessel, hence there is a vertical distance of 33.3 cm between the downcomer outlet and the bottom of the flotation column.

2.2. *Three phases and suspension*

We assume that the attachment of solid hydrophobic particles to bubbles (aggregation) occurs only in the inlet pipe and is completed before the mixture is fed into the column. For the mathematical modelling inside the column, we introduce three phases: the *fluid phase*, the *solid phase*, which models solid particles that are suspended in the fluid, and the *aggregate phase*, which models gas bubbles fully loaded with hydrophobic particles. Variables are correspondingly indexed by f, s and a. By *suspension* we mean the union of the solid and fluid phases. We let $\phi_i = \phi_i(z,t)$ denote the volume fraction of phase $i \in \{\mathrm{a},\mathrm{f},\mathrm{s}\}$ and assume that the three phases fill out the flotation column; $\phi_{\mathrm{a}} + \phi_{\mathrm{f}} + \phi_{\mathrm{s}} \equiv 1$. When the final form of the governing equation has been derived we will use the simpler notation $\phi := \phi_{\mathrm{a}}$; cf. (1.1).

We assume constant phase densities $\rho_{\mathrm{a}} < \rho_{\mathrm{f}} < \rho_{\mathrm{s}}$, consistently with the assumption that bubbles rise (float) and particles settle (sink). This simplification can be discussed, since the hydrophobic and hydrophilic particles often have different densities. Introducing two different solid phases would lead to the additional modelling problem of sedimentation of a binary suspension, which we postpone for future analysis. Modelling only one solid phase can nevertheless be of interest. If the volumetric flows of gas and slurry are adjusted carefully so that all hydrophobic particles are attached to bubbles, then there are only hydrophilic particles (gangue) left in the suspension. This is in fact the purpose of the process. It is then of interest to model the sedimentation of the gangue to predict under what conditions this is removed through the tailings underflow and not caught by the upstream.

For the constitutive assumptions to be presented later, the aggregate bubbles and the solid particles are assumed to be monosized. We also suppose that gas bubbles do not coalesce or break.

2.3. *Conservation laws of the three phases*

Conservation of mass for each phase implies the system of balance equations

$$\frac{\partial}{\partial t}\big(A(z)\phi_{\mathrm{a}}\big) + \frac{\partial}{\partial z}\big(A(z)\phi_{\mathrm{a}}v_{\mathrm{a}}\big) = Q_{\mathrm{F}}\phi_{\mathrm{a,F}}\delta_{z_{\mathrm{F}}}, \tag{2.2}$$

$$\frac{\partial}{\partial t}\big(A(z)\phi_{\mathrm{s}}\big) + \frac{\partial}{\partial z}\big(A(z)\phi_{\mathrm{s}}v_{\mathrm{s}}\big) = Q_{\mathrm{F}}\phi_{\mathrm{s,F}}\delta_{z_{\mathrm{F}}}, \tag{2.3}$$

$$\frac{\partial}{\partial t}\big(A(z)\phi_{\mathrm{f}}\big) + \frac{\partial}{\partial z}\big(A(z)\phi_{\mathrm{f}}v_{\mathrm{f}}\big) = Q_{\mathrm{F}}\phi_{\mathrm{f,F}}\delta_{z_{\mathrm{F}}} + Q_{\mathrm{W}}\phi_{\mathrm{f,W}}\rho_{\mathrm{f}}\delta_{z_{\mathrm{W}}}, \tag{2.4}$$

where the right-hand sides contain Dirac functions, volumetric flows and the incoming volume fractions of aggregates $\phi_{\mathrm{a,F}}$, solids $\phi_{\mathrm{s,F}}$ and fluid $\phi_{\mathrm{f,W}} \equiv 1$. At the feed inlet we assume that $\phi_{\mathrm{a,F}} + \phi_{\mathrm{s,F}} + \phi_{\mathrm{f,F}} \equiv 1$ with $0 < \phi_{\mathrm{a,F}}, \phi_{\mathrm{s,F}}, \phi_{\mathrm{f,F}} < 1$.

We define the volume-average velocity, or bulk velocity, of the mixture by

$$q := \phi_{\mathrm{a}}v_{\mathrm{a}} + \phi_{\mathrm{s}}v_{\mathrm{s}} + \phi_{\mathrm{f}}v_{\mathrm{f}} \tag{2.5}$$

and replace (2.4) by the sum of (2.2)–(2.4), which is

$$\frac{\partial}{\partial z}\big(A(z)q\big) = Q_{\mathrm{F}}\delta_{z_{\mathrm{F}}} + Q_{\mathrm{W}}\delta_{z_{\mathrm{W}}}. \tag{2.6}$$

Consequently, in the flotation column q varies with height z because of the two inlet flows and the two values of the cross-sectional area. In view of (2.1) and since $A(z)q(z,t) = -Q_{\mathrm{U}}(t)$ for $z < z_{\mathrm{F}}$, we can integrate (2.6) to obtain

$$q(z,t) = \begin{cases} q_1 := -Q_{\mathrm{U}}/A_{\mathrm{U}} & \text{for } z < z_{\mathrm{F}}, \\ q_2 := (-Q_{\mathrm{U}} + Q_{\mathrm{F}})/A_{\mathrm{E}} & \text{for } z_{\mathrm{F}} \le z < z_{\mathrm{W}}, \\ q_3 := (-Q_{\mathrm{U}} + Q_{\mathrm{F}} + Q_{\mathrm{W}})/A_{\mathrm{E}} & \text{for } z \ge z_{\mathrm{W}}. \end{cases}$$

Hence, this identity replaces (2.4), and we will next rewrite the fluxes in the remaining PDEs (2.2) and (2.3) in terms of q and two constitutive functions.

2.4. *Convective fluxes expressed in terms of constitutive functions*

The drift-flux and the solids-flux theories are given by a batch-drift-flux function $j_{\mathrm{b}}(\phi_{\mathrm{a}})$ and a batch-settling-flux function $f_{\mathrm{b}}(\varphi)$, respectively. Here φ is the volume fraction of solids within the suspension:

$$\varphi := \frac{\phi_{\mathrm{s}}}{\phi_{\mathrm{s}} + \phi_{\mathrm{f}}} = \frac{\phi_{\mathrm{s}}}{1 - \phi_{\mathrm{a}}}. \tag{2.7}$$

We denote the volume-average velocity, or bulk velocity, of the suspension by

$$q_{\mathrm{sus}} := \frac{\phi_{\mathrm{s}}v_{\mathrm{s}} + \phi_{\mathrm{f}}v_{\mathrm{f}}}{\phi_{\mathrm{s}} + \phi_{\mathrm{f}}} = \varphi v_{\mathrm{s}} + \frac{1 - \phi_{\mathrm{a}} - \phi_{\mathrm{s}}}{1 - \phi_{\mathrm{a}}}v_{\mathrm{f}} = \varphi v_{\mathrm{s}} + (1 - \varphi)v_{\mathrm{f}}.$$

Then we define the aggregate-suspension relative velocity

$$u_{\mathrm{asus}} := v_{\mathrm{a}} - q_{\mathrm{sus}} = v_{\mathrm{a}} - \varphi v_{\mathrm{s}} - (1 - \varphi)v_{\mathrm{f}} \tag{2.8}$$

and the solid-fluid relative velocity

$$u_{\mathrm{sf}} := v_{\mathrm{s}} - v_{\mathrm{f}}. \tag{2.9}$$

We will express the two PDEs (2.2) and (2.3) in terms of the velocities q, u_{asus} and u_{sf}, and the unknowns ϕ_{a} and φ. Using (2.5), (2.7), (2.8) and (2.9), we obtain the following expressions for the phase velocities v_{a} and v_{s} in terms of the bulk velocity q and the relative velocities u_{asus} and u_{sf}:

$$v_{\mathrm{a}} = q + (1 - \phi_{\mathrm{a}})u_{\mathrm{asus}}, \quad v_{\mathrm{s}} = q + (1 - \varphi)u_{\mathrm{sf}} - \phi_{\mathrm{a}}u_{\mathrm{asus}}.$$

We now define the relative velocities in terms of the constitutive functions by

$$\phi_{\mathrm{a}}(1-\phi_{\mathrm{a}})u_{\mathrm{asus}} =: j_{\mathrm{b}}(\phi_{\mathrm{a}}), \tag{2.10}$$

$$\varphi(1-\varphi)u_{\mathrm{sf}} =: -f_{\mathrm{b}}(\varphi), \tag{2.11}$$

where $f_{\mathrm{b}} \geq$ in the downwards direction of sedimentation. Then we get the following expressions for the total fluxes of (2.2) and (2.3):

$$\begin{aligned}
\phi_{\mathrm{a}}v_{\mathrm{a}} &= \phi_{\mathrm{a}}q + j_{\mathrm{b}}(\phi_{\mathrm{a}}) =: J(\phi_{\mathrm{a}}, z, t),\\
\phi_{\mathrm{s}}v_{\mathrm{s}} &= (1-\phi_{\mathrm{a}})\varphi q - (1-\phi_{\mathrm{a}})f_{\mathrm{b}}(\varphi) - \varphi j_{\mathrm{b}}(\phi_{\mathrm{a}}) =: -F(\varphi, \phi_{\mathrm{a}}, z, t),
\end{aligned}$$

where the minus sign is to have F positive in the direction of sedimentation. Inserting these expressions into (2.2) and (2.3) we get the governing PDE system (1.1) with the shorter notation $\phi := \phi_{\mathrm{a}}$, which will be used in the rest of this paper.

In the under- and overflow zones, all three phases are assumed to have the same velocity, i.e., u_{asus} and u_{sf} are zero, which means that we set $j_{\mathrm{b}} := 0$ and $f_{\mathrm{b}} := 0$ in those zones. The total flux functions in (1.1) are thus given by

$$J(\phi, z, t) = \begin{cases}
j_{\mathrm{E}}(\phi, t) := q_3(t)\phi & \text{for } z \geq z_{\mathrm{E}},\\
j_3(\phi, t) := q_3(t)\phi + j_{\mathrm{b}}(\phi) & \text{for } z_{\mathrm{W}} \leq z < z_{\mathrm{E}},\\
j_2(\phi, t) := q_2(t)\phi + j_{\mathrm{b}}(\phi) & \text{for } z_{\mathrm{F}} \leq z < z_{\mathrm{W}},\\
j_1(\phi, t) := q_1(t)\phi + j_{\mathrm{b}}(\phi) & \text{for } z_{\mathrm{U}} \leq z < z_{\mathrm{F}},\\
j_{\mathrm{U}}(\phi, t) := q_1(t)\phi & \text{for } z < z_{\mathrm{U}},
\end{cases}$$

$$F(\varphi, \phi, z, t) = \begin{cases}
f_{\mathrm{E}}(\varphi, \phi, t) := -(1-\phi)q_3(t)\varphi & \text{for } z \geq z_{\mathrm{E}},\\
f_3(\varphi, \phi, t) & \text{for } z_{\mathrm{W}} \leq z < z_{\mathrm{E}},\\
f_2(\varphi, \phi, t) & \text{for } z_{\mathrm{F}} \leq z < z_{\mathrm{W}},\\
f_1(\varphi, \phi, t) & \text{for } z_{\mathrm{U}} \leq z < z_{\mathrm{F}},\\
f_{\mathrm{U}}(\varphi, \phi, t) := -(1-\phi)q_1(t)\varphi & \text{for } z < z_{\mathrm{U}},
\end{cases}$$

where

$$\begin{aligned}
f_k(\varphi, \phi, t) &:= (1-\phi)f_{\mathrm{b}}(\varphi) + \big(j_{\mathrm{b}}(\phi) - (1-\phi)q_k(t)\big)\varphi\\
&= (1-\phi)f_{\mathrm{b}}(\varphi) + \big(j_k(\phi, t) - q_k(t)\big)\varphi, \quad k = 1, 2, 3.
\end{aligned} \tag{2.12}$$

2.5. *Constitutive flux functions for rising aggregates and settling particles*

Inside the flotation column, the relative velocities of rising aggregate bubbles relative to the suspension, u_{asus}, and settling particles relative to the fluid, u_{sf} (negative according to the upwards-pointing z-axis), are expressed by constitutive functions, namely the drift-flux function j_{b} and the settling-flux function f_{b} (see (2.10) and (2.11)). Both functions are assumed to depend on one variable, to be non-negative, continuously differentiable, and unimodal, to satisfy $j_{\mathrm{b}}(0) = j_{\mathrm{b}}(1) = 0$ and $f_{\mathrm{b}}(0) =$

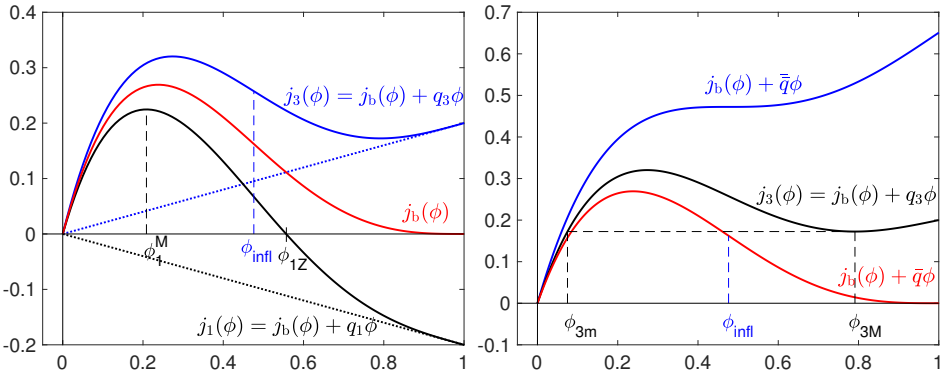

Fig. 2. Properties of flux functions and specific volume fractions. Left: Drift-flux function j_b and flux curves for zones 1 and 3. Right: The local minimum ϕ_M and appurtenant ϕ_m for a zone flux j with positive q, and flux curves with zero derivatives at $\phi_{max} = 1$ and ϕ_{infl}. In these and other plots, we have used the expression (2.15) with $n_{asus} = 3.2$ in the drift-flux function j_b. The unit on the vertical axis is cm/s.

$f_b(1) = 0$, and to have precisely one inflection point, ϕ_{infl} and φ_{infl}, respectively, to the right of the respective maximum point; see Fig. 2.

Moreover, we assume that

$$j_b(\phi) = \phi(1-\phi)u_{asus}(\phi) = \phi v_{term,a} V_{asus}(\phi), \tag{2.13}$$
$$f_b(\varphi) = -\varphi(1-\varphi)u_{sf}(\varphi) = \varphi v_{term,s} V_{sf}(\varphi), \tag{2.14}$$

where $v_{term,a}$ and $v_{term,s}$ are the terminal velocities of a single aggregate and a single solid particle, respectively, in an unbounded fluid. There exists a number of methods to calculate the terminal velocities. Wallis' generalized correlation[48] is recommended and used in this work; see Ref. 43 (Appendix A) for details. This correlation involves additional quantities such as equilibrium surface tension and the viscosity of the fluid. Its discussion is beyond our focus; here it suffices to assume that $v_{term,a} > 0$ and $v_{term,s} > 0$ are set constants for a given material.

Furthermore, $V_{asus}(\phi)$ and $V_{sf}(\varphi)$ are dimensionless hindered-bubbling and hindered-settling functions satisfying $V_{asus}(0) = V_{sf}(0) = 1$. They are often given by the Richardson-Zaki expression[39]

$$\begin{aligned} V_{asus}(\phi) &= (1-\phi)^{n_{asus}}, \quad n_{asus} \geq 0, \quad \phi \in [0, \phi_{max}], \\ V_{sf}(\varphi) &= (1-\varphi)^{n_{sf}}, \quad n_{sf} \geq 1, \quad \varphi \in [0, \varphi_{max}]. \end{aligned} \tag{2.15}$$

The maximum possible volume fractions are $\phi_{max} = \varphi_{max} = 1$. Realistic values of n_{asus} range from 2 to 3.2 (cf., e.g., Refs 16, 28, 38, 46). We use $n_{asus} = 3.2$ and $v_{term,a} = 2.7\,\mathrm{cm/s}$ for all plots and simulations in the present article. For the batch-settling flux f_b, we use $n_{sf} = 2.5$ (cf., e.g., Ref. 16) and $v_{term,s} = 0.5\,\mathrm{cm/s}$.

2.6. *Properties of the zone flux functions*

The properties of the functions j_b and f_b are qualitatively the same. We have $j_\mathrm{b}(0) = j_\mathrm{b}(1) = 0$, $f_\mathrm{b}(0) = f_\mathrm{b}(1) = 0$, and there are inflection points $\phi_\mathrm{infl} \in (0,1)$ (see Fig. 2) and $\varphi_\mathrm{infl} \in (0,1)$. The zone flux functions (for aggregates or solids) have also an additional linear term due to the bulk velocity of the zone. We suppress the t-variable when considering steady states, and let $j(\phi) = j_\mathrm{b}(\phi) + q\phi$ denote a zone flux function. The case for the settling zone flux function $f(\cdot,\phi)$ is similar; however, with an additional dependence on ϕ. As will be seen, any steady-state solution can have at most two constant states of ϕ in each zone.

The form of j_b singles out certain distinguished values of the volume fraction that appear in the steady-state solution (see Fig. 2). For $f(\cdot,\phi)$, the analogous distinguished values depend also on the local value of ϕ. This will be clear in the specific cases of steady states.

The inflection point ϕ_infl of j is independent of q, but other distinguished values depend on q. If $j(\phi)$ has a zero in $(0,1)$, which can happen only for $q < 0$, then we denote it by $\phi_\mathrm{Z} = \phi_\mathrm{Z}(q)$. If $j(\phi) < 0$ for all $\phi \in (0,1]$, we set $\phi_\mathrm{Z} := 0$. We define

$$\bar{q} := -j_\mathrm{b}'(1), \qquad \bar{\bar{q}} := -j_\mathrm{b}'(\phi_\mathrm{infl}),$$

which are the bulk velocities such that the derivative of $j(\phi)$ is zero at $\phi_\mathrm{max} = 1$ and ϕ_infl, respectively. To reduce the number of cases for steady-state solutions, we assume (as we did in Ref. 8) that

$$\bar{q} = -j_\mathrm{b}'(1) = 0,$$

in accordance with the common Richardson-Zaki function (2.15). For $\bar{q} < q < \bar{\bar{q}}$, there is a local minimizer ϕ_M of $j(\phi)$ on the right of ϕ_infl. Then $0 = j'(\phi_\mathrm{M}) = j_\mathrm{b}'(\phi_\mathrm{M}) + q$. To obtain a definition of ϕ_M for all values of q, we note that the restriction $(j_\mathrm{b}|_{(\phi_\mathrm{infl},1)})'$ is an increasing function so that we can define

$$\phi_\mathrm{M} = \phi_\mathrm{M}(q) := \begin{cases} 1 & \text{if } q \le \bar{q}, \\ ((j_\mathrm{b}|_{(\phi_\mathrm{infl},1)})')^{-1}(-q) & \text{if } \bar{q} < q < \bar{\bar{q}}, \\ \phi_\mathrm{infl} & \text{if } q \ge \bar{\bar{q}}. \end{cases}$$

Given ϕ_M and $q \ge 0$, we define $\phi_\mathrm{m} = \phi_\mathrm{m}(q)$ as the unique value satisfying

$$j(\phi_\mathrm{m}) = j(\phi_\mathrm{M}), \quad 0 \le \phi_\mathrm{m} \le \phi_\mathrm{infl}.$$

For $q < \bar{\bar{q}}$, $j(\phi)$ assumes a local maximum at $\phi^\mathrm{M} \in [0, \phi_\mathrm{infl})$. Let $q_\mathrm{neg} := -j_\mathrm{b}'(0)$ be the value below which j is a decreasing function. For $q \le q_\mathrm{neg}$, the local maximum is $\phi^\mathrm{M} := 0$. For $q \ge \bar{\bar{q}}$, we set $\phi^\mathrm{M} := \phi_\mathrm{infl}$.

In many instances it is convenient to write out the dependence on q also of the flux function, i.e. $j(\phi; q)$. From the definitions above (cf. Ref. 19, Lemma 2) we obtain the following properties:

Lemma 2.1. *The following properties hold:*

$$\phi'_{\mathrm{M}}(q)\begin{cases}=0 & \text{if } q<\bar{q},\\ <0 & \text{if } \bar{q}<q<\bar{\bar{q}},\\ =0 & \text{if } q>\bar{\bar{q}},\end{cases}\qquad (\phi^{\mathrm{M}})'(q)\begin{cases}=0 & \text{if } q<q_{\mathrm{neg}},\\ >0 & \text{if } q_{\mathrm{neg}}<q<\bar{\bar{q}},\\ =0 & \text{if } q>\bar{\bar{q}},\end{cases}$$

$$\frac{\mathrm{d}}{\mathrm{d}q}j\big(\phi_{\mathrm{M}}(q);q\big)=\phi_{\mathrm{M}}(q),\qquad \frac{\mathrm{d}}{\mathrm{d}q}j\big(\phi^{\mathrm{M}}(q);q\big)=\phi^{\mathrm{M}}(q).$$

For the specific zone flux functions j_k, $k=1,2,3$, we use the notation $\phi_{k\mathrm{M}}=\phi_{\mathrm{M}}(q_k)$, etc.

2.7. *A comment on the triangular hyperbolic system and entropy solutions*

The governing equations for the conservative variables $\phi:=\phi_{\mathrm{a}}$ and ϕ_{s} inside the column are the following:

$$\frac{\partial}{\partial t}\left(A(z)\begin{pmatrix}\phi\\ \phi_{\mathrm{s}}\end{pmatrix}\right)+\frac{\partial}{\partial z}\left(A(z)\begin{pmatrix}J(\phi,z,t)\\ -F(\phi_{\mathrm{s}}/(1-\phi),\phi,z,t))\end{pmatrix}\right)=Q_{\mathrm{F}}(t)\begin{pmatrix}\phi_{\mathrm{F}}(t)\\ \phi_{\mathrm{s,F}}(t)\end{pmatrix}\delta_{z_{\mathrm{F}}}. \tag{2.16}$$

Inside a zone where $A\equiv$ constant and there is no source term, the triangular system (2.16) is non-trivial to analyse. It is non-strictly hyperbolic since the difference of the eigenvalues λ_ϕ and $\lambda_{\phi_{\mathrm{s}}}$ of the Jacobian, which is

$$\lambda_\phi-\lambda_{\phi_{\mathrm{s}}}=q+j'_{\mathrm{b}}(\phi)-\left(q-f'_{\mathrm{b}}(\varphi)-\frac{j_{\mathrm{b}}(\phi)}{1-\phi}\right)=j'_{\mathrm{b}}(\phi)+\frac{j_{\mathrm{b}}(\phi)}{1-\phi}+f'_{\mathrm{b}}(\varphi),$$

may have any sign by the following argument. All three terms are positive for small ϕ and φ. For large φ, the third term is negative and for the common drift-flux function $j_{\mathrm{b}}(\phi)=C\phi(1-\phi)^n$, the sum of the first two terms is $(1-\phi)^{n-1}(1-n\phi)$, which is also negative for $\phi>1/n$. Furthermore, the eigenvector $\boldsymbol{r}_\phi=(1,0)^{\mathrm{T}}$ implies that $\nabla\lambda_\phi\cdot\boldsymbol{r}_\phi=-j''_{\mathrm{b}}(\phi)$, which may have any sign, so this field is not genuinely nonlinear.

The equation for ϕ of (1.1) does not contain the unknown φ. Hence, this equation can in principle be solved first for a desired time period by the method of characteristics and the theory for scalar conservation laws with discontinuous flux function. When ϕ is a known function, the second equation of (1.1) can in principle be solved for φ by the same scalar theory. The system (1.1) can therefore be analysed by the theory of a scalar conservation law with discontinuous flux function.

Within each zone, where we assume that the cross-sectional area A is constant, the governing equation has the form $\phi_t+g(\phi)_\xi=0$ for some flux function g, and we consider the Cauchy problem for this equation. A piecewise smooth function $\phi=\phi(\xi,t)$ is said to be an *entropy solution* if ϕ is continuously differentiable everywhere except along a finite number of curves $\xi=\xi_{\mathrm{d}}(t)\in C^1$ of discontinuities, where the following two conditions are satisfied. At each point $(\xi_{\mathrm{d}}(t),t)$ of discontinuity, the

(non-equal) values $\phi^{\pm} := \phi(\xi_{\mathrm{d}}(t)^{\pm}, t)$ satisfy the jump condition

$$\xi_{\mathrm{d}}'(t) = S(\phi^+, \phi^-) := \frac{g(\phi^+) - g(\phi^-)}{\phi^+ - \phi^-}, \tag{2.17}$$

and the jump entropy condition

$$S(u, \phi^-) \geq S(\phi^+, \phi^-) \quad \text{for all } u \text{ between } \phi^+ \text{ and } \phi^-. \tag{2.18}$$

It is well known that entropy solutions in the sense of Oleinik[37] are also the unique entropy solutions in the sense of Kružkov-type[32,34] integral inequalities. On the other hand, at the spatial discontinuities of each of the equations in (1.1), a generalized entropy is needed.[17,21,33] Since we only construct steady-state solutions, we review that condition next for this purpose, which means less notation than for the transient case.

2.8. *Construction of steady-state solutions for a conservation law with discontinuous flux*

Consider the Riemann problem for a scalar conservation law with discontinuous flux function:

$$\frac{\partial \phi}{\partial t} + \frac{\partial}{\partial \xi}\big((1 - H_{\xi_0}) g_{\mathrm{L}}(\phi) + H_{\xi_0} g_{\mathrm{R}}(\phi)\big) = 0,$$

$$\phi(\xi, t) = \begin{cases} \phi_- & \text{if } \xi < \xi_0, \\ \phi_+ & \text{if } \xi > \xi_0, \end{cases}$$

where $H_{\xi_0}(\xi) := H(\xi - \xi_0)$ is the Heaviside function with a jump at $\xi = \xi_0$ and $\phi_{\pm}$ are constants. This Cauchy problem should be interpreted in the weak sense and we seek steady-state solutions. The conservation law across $\xi = \xi_0$ implies the jump condition $g_{\mathrm{L}}(\phi_-) = g_{\mathrm{R}}(\phi_+)$ (see (2.17)). This single equation has two unknowns. The generalized entropy condition[17] selects the physically relevant solution in a neighbourhood of $\xi = \xi_0$ for a dynamic solution. We define the auxiliary functions

$$\hat{g}_{\mathrm{R}}(\phi; \phi_+) := \begin{cases} \min\limits_{v \in [\phi, \phi_+]} g_{\mathrm{R}}(v) & \text{if } \phi \leq \phi_+, \\ \max\limits_{v \in [\phi_+, \phi]} g_{\mathrm{R}}(v) & \text{if } \phi > \phi_+, \end{cases}$$

$$\check{g}_{\mathrm{L}}(\phi; \phi_-) := \begin{cases} \max\limits_{v \in [\phi, \phi_-]} g_{\mathrm{L}}(v) & \text{if } \phi \leq \phi_-, \\ \min\limits_{v \in [\phi_-, \phi]} g_{\mathrm{L}}(v) & \text{if } \phi > \phi_-. \end{cases}$$

Since $\check{g}_{\mathrm{L}}(\cdot; \phi_-)$ is non-increasing and $\hat{g}_{\mathrm{R}}(\cdot; \phi_+)$ is non-decreasing, the intersection of the graphs of these functions occurs at a unique flux value, if an intersection exists. For the model of bubble concentrations in a flotation column in Ref. 8, corresponding to the first equation of (1.1), this is always the case; this statement can be proven in the same way as for the problem of continuous sedimentation;

see Ref. 18. This will also follow from the construction of steady states in Section 3. The analogous situation holds for the constructed steady states for φ in Section 4.

We define the set of ϕ-values of the intersection of $\check{g}_{\mathrm{L}}(\cdot;\phi_-)$ and $\hat{g}_{\mathrm{R}}(\cdot;\phi_+)$ as

$$\bar{\Phi} = \bar{\Phi}(\phi_+,\phi_-) := \big\{\phi\in[0,1] : \hat{g}_{\mathrm{R}}(\phi;\phi_+) = \check{g}_{\mathrm{L}}(\phi;\phi_-)\big\}$$

and the corresponding unique flux value $\eta(\phi_+,\phi_-) := \hat{g}_{\mathrm{R}}(\bar{\Phi};\phi_+)$. Since we are here only interested in stationary solutions, the generalized entropy condition can be stated as

$$\hat{g}_{\mathrm{R}}(\phi_+;\phi_+) = \eta(\phi_+,\phi_-) = \check{g}_{\mathrm{L}}(\phi_-;\phi_-), \tag{2.19}$$

where we note that $\hat{g}_{\mathrm{R}}(\phi_+;\phi_+) = g_{\mathrm{R}}(\phi_+)$ and $\check{g}_{\mathrm{L}}(\phi_-;\phi_-) = g_{\mathrm{L}}(\phi_-)$.

3. Construction of steady states for the aggregate phase

The steady states of scalar conservation laws with discontinuous flux are stationary (time-independent) solutions, which are piecewise constant functions of z. We consider first the case when ϕ is constant in each zone. This will be done here for the first equation of (1.1):

$$\frac{\partial}{\partial t}\big(A(z)\phi\big) + \frac{\partial}{\partial z}\big(A(z)J(\phi,z,t)\big) = Q_{\mathrm{F}}(t)\phi_{\mathrm{F}}(t)\delta_{z_{\mathrm{F}}}, \tag{3.1}$$

which models the situation when gas and feed slurry are fed at the same location (see Fig. 1), in contrast to the scenario studied in Ref. 8. The constant steady-state solutions in the five zones are denoted by ϕ_{U}, ϕ_1, ϕ_2, ϕ_3 and ϕ_{E}. We deal with possible discontinuities within a zone in Section 3.4.

3.1. *Couplings at the outflow locations $z = z_{\mathrm{U}}$ and $z = z_{\mathrm{E}}$*

This case is treated in Ref. 8 and the outcome is that the possible steady-state values in zones 1 and 3, the underflow zone, and the effluent zone are

$$\phi_1 \in \{0\}\cup[\phi_{1\mathrm{Z}},1], \quad \phi_3 \in [0,\phi_{3\mathrm{m}}]\cup[\phi_{3\mathrm{M}},1], \tag{3.2}$$

$$\phi_{\mathrm{U}} = -\frac{A_{\mathrm{U}}j_1(\phi_1)}{Q_{\mathrm{U}}}, \quad \phi_{\mathrm{E}} = \frac{A_{\mathrm{E}}j_3(\phi_3)}{Q_{\mathrm{E}}}. \tag{3.3}$$

3.2. *Couplings at $z = z_{\mathrm{F}}$*

Near $z = z_{\mathrm{F}}$ and setting $S_{\mathrm{F}} := Q_{\mathrm{F}}\phi_{\mathrm{F}} > 0$, we obtain from Equation (3.1)

$$A(z)\frac{\partial\phi}{\partial t} + \frac{\partial}{\partial z}\big((1-H_{z_{\mathrm{F}}})A_{\mathrm{U}}j_1(\phi,t) + H_{z_{\mathrm{F}}}A_{\mathrm{E}}j_2(\phi,t)\big) = S_{\mathrm{F}}\delta_{z_{\mathrm{F}}}. \tag{3.4}$$

With the identity $-\delta_{z_{\mathrm{F}}} = \partial(1-H_{z_{\mathrm{F}}})/\partial z$, (3.4) is formally equivalent to

$$A(z)\frac{\partial\phi}{\partial t} + \frac{\partial}{\partial z}\Big((1-H_{z_{\mathrm{F}}})\big(A_{\mathrm{U}}j_1(\phi,t)+S_{\mathrm{F}}\big) + H_{z_{\mathrm{F}}}A_{\mathrm{E}}j_2(\phi,t)\Big) = 0.$$

Thus, the flux functions to consider for the steady-state coupling between ϕ_1 and ϕ_2 are the following, where we refer to the notation of Section 2.8:

$$g_{\mathrm{L}}(\phi) = A_{\mathrm{U}} j_1(\phi) + S_{\mathrm{F}} = A_{\mathrm{U}} j_{\mathrm{b}}(\phi) - Q_{\mathrm{U}}\phi + S_{\mathrm{F}} \quad \text{for } z < z_{\mathrm{F}}, \tag{3.5}$$

$$g_{\mathrm{R}}(\phi) = A_{\mathrm{E}} j_2(\phi) = A_{\mathrm{E}} j_{\mathrm{b}}(\phi) - Q_{\mathrm{U}}\phi + Q_{\mathrm{F}}\phi \qquad \text{for } z > z_{\mathrm{F}}. \tag{3.6}$$

Lemma 3.1. *The continuous functions g_{L} and g_{R} given by* (3.5) *and* (3.6) *intersect at the unique volume fraction $\phi_{1,2}^{\mathrm{int}} \in (0,1)$, which is defined by*

$$(A_{\mathrm{U}} - A_{\mathrm{E}}) j_{\mathrm{b}}(\phi_{1,2}^{\mathrm{int}}) = Q_{\mathrm{F}}(\phi_{1,2}^{\mathrm{int}} - \phi_{\mathrm{F}}). \tag{3.7}$$

Furthermore, $g_{\mathrm{L}}(\phi_1^{\mathrm{M}}) > g_{\mathrm{R}}(\phi_2^{\mathrm{M}})$.

Proof. We may write (3.7) as $d_1(\phi_{1,2}^{\mathrm{int}}) = 0$, where $d_1(\phi) := g_{\mathrm{L}}(\phi) - g_{\mathrm{R}}(\phi)$ satisfies $d_1(0) = S_{\mathrm{F}} > 0$, $d(1) = Q_{\mathrm{F}}(\phi_{\mathrm{F}} - 1) < 0$ and $d_1''(\phi) = (A_{\mathrm{U}} - A_{\mathrm{E}}) j_{\mathrm{b}}''(\phi)$, which means that d_1 has the same concave-convex behaviour as j_{b}. It follows that there exists a unique intersection in $(0,1)$. For any fixed Q_{F}, we analyse the difference

$$d_2(Q_{\mathrm{U}}) := g_{\mathrm{L}}(\phi^{\mathrm{M}}(q_1); q_1) - g_{\mathrm{R}}(\phi^{\mathrm{M}}(q_2); q_2), \quad Q_{\mathrm{U}} \geq 0,$$

where $q_1 = -Q_{\mathrm{U}}/A_{\mathrm{U}} < q_2 = (Q_{\mathrm{F}} - Q_{\mathrm{U}})/A_{\mathrm{E}}$. We have $d_2(0) = S_{\mathrm{F}} > 0$ and

$$\begin{aligned} d_2'(Q_{\mathrm{U}}) &= A_{\mathrm{U}} \frac{\mathrm{d}}{\mathrm{d}q_1} j_1(\phi^{\mathrm{M}}(q_1); q_1) \left(-\frac{1}{A_{\mathrm{U}}}\right) - A_{\mathrm{E}} \frac{\mathrm{d}}{\mathrm{d}q_2} j_2(\phi^{\mathrm{M}}(q_2); q_2) \left(-\frac{1}{A_{\mathrm{E}}}\right) \\ &= -\phi^{\mathrm{M}}(q_1) + \phi^{\mathrm{M}}(q_2) \geq 0, \end{aligned}$$

because of Lemma 2.1. □

The entropy condition (2.19) is in this case

$$A_{\mathrm{E}} \hat{\jmath}_2(\phi_2; \phi_2) = \eta(\phi_1, \phi_2) = A_{\mathrm{U}} \check{\jmath}_1(\phi_1; \phi_1) + S_{\mathrm{F}} \tag{3.8}$$

and, in particular, the jump condition is

$$A_{\mathrm{E}} j_2(\phi_2;) = A_{\mathrm{U}} j_1(\phi_1) + S_{\mathrm{F}}. \tag{FJC}$$

We have $q_1 = -Q_{\mathrm{U}}/A_{\mathrm{U}} \leq 0$, but q_2 may have any sign. A steady state in zone 1 satisfies $\phi_1 \in \{0\} \cup [\phi_{1\mathrm{Z}}, 1]$. The corresponding two qualitatively different $\check{g}_{\mathrm{L}}(\cdot; \phi_1)$ should be coupled with the three possibilities of $\hat{g}_{\mathrm{R}}(\cdot; \phi_2)$, when ϕ_2 belongs to the monotonicity intervals of g_{R}, which are separated by ϕ_2^{M} and $\phi_{2\mathrm{M}}$.

For $q_2 \geq 0$, the possible couplings are the following, where we purposely have overlapping boundary cases to minimize the number of necessary conditions:

(a) $\phi_1 = 0$, $\phi_2 \in [0, \phi_2^{\mathrm{M}}]$; see Fig. 3(a), which shows that the plateau of $\check{g}_{\mathrm{L}}$ intersects the leftmost increasing part of $\hat{g}_{\mathrm{R}}$. Then ϕ_2 is uniquely defined by the jump condition (FJC) and necessary conditions on the volumetric flows are

$$A_{\mathrm{E}} j_2(\phi_2^{\mathrm{M}}) \geq S_{\mathrm{F}}. \tag{FIa}$$

$$\phi_2 \leq \phi_{1\mathrm{Z}}, \quad \text{where } \phi_2 \leq \phi_2^{\mathrm{M}} \text{ is defined by } A_{\mathrm{E}} j_2(\phi_2) = S_{\mathrm{F}}. \tag{FIb}$$

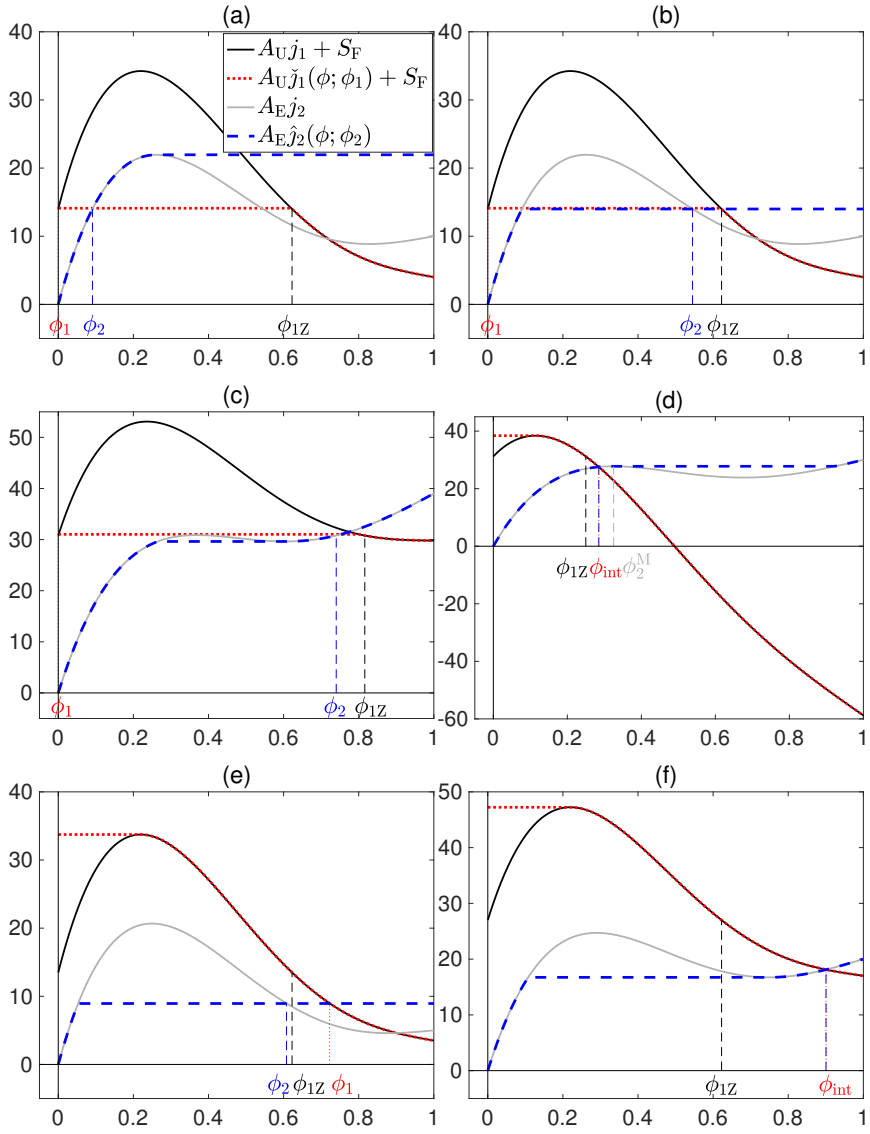

Fig. 3. Couplings at z_{F} for (a), (b) $Q_{\mathrm{U}} = 10\,\mathrm{cm}^3/\mathrm{s}$, $\phi_{\mathrm{F}} = 0.7$ and $Q_{\mathrm{F}} = 20\,\mathrm{cm}^3/\mathrm{s}$, with $Q_2 = -Q_{\mathrm{U}} + Q_{\mathrm{F}}$, (c) $Q_{\mathrm{U}} = 1\,\mathrm{cm}^3/\mathrm{s}$, $\phi_{\mathrm{F}} = 0.77$ and $Q_{\mathrm{F}} = 40\,\mathrm{cm}^3/\mathrm{s}$, (d) $Q_{\mathrm{U}} = 90\,\mathrm{cm}^3/\mathrm{s}$, $\phi_{\mathrm{F}} = 0.26$ and $Q_{\mathrm{F}} = 120\,\mathrm{cm}^3/\mathrm{s}$, (e) $Q_{\mathrm{U}} = 10\,\mathrm{cm}^3/\mathrm{s}$, $\phi_{\mathrm{F}} = 0.9$ and $Q_{\mathrm{F}} = 15\,\mathrm{cm}^3/\mathrm{s}$, (f) $Q_{\mathrm{U}} = 10\,\mathrm{cm}^3/\mathrm{s}$, $\phi_{\mathrm{F}} = 0.9$ and $Q_{\mathrm{F}} = 30\,\mathrm{cm}^3/\mathrm{s}$.

(b) $\phi_1 = 0$, $\phi_2 \in [\phi_2^{\mathrm{M}}, \phi_{2\mathrm{M}}]$; see Fig. 3(b), which shows that the plateau of $\check{g}_{\mathrm{L}}$ intersects the plateau of $\hat{g}_{\mathrm{R}}$. Necessary conditions are (FIa) and

$$A_{\mathrm{E}}j_2(\phi_{2\mathrm{M}}) \le S_{\mathrm{F}}, \tag{FIIa}$$

$$\phi_2 \le \phi_{1\mathrm{Z}}, \quad \text{where } \phi_2 \in [\phi_2^{\mathrm{M}}, \phi_{2\mathrm{M}}] \text{ is the solution of } A_{\mathrm{E}} j_2(\phi_2) = S_{\mathrm{F}}. \quad \text{(FIIb)}$$

(c) $\phi_1 = 0$, $\phi_2 \in [\phi_{2\mathrm{M}}, 1]$; see Fig. 3(c), which shows that the plateau of $\check{g}_{\mathrm{L}}$ intersects the rightmost increasing part of $\hat{g}_{\mathrm{R}}$. A coupling is possible only if condition (FIIa) and the following are satisfied:

$$A_{\mathrm{E}} j_2(1) \ge S_{\mathrm{F}} \quad \Leftrightarrow \quad Q_{\mathrm{F}}(1-\phi_{\mathrm{F}}) \ge Q_{\mathrm{U}}, \quad \text{(FIIIa)}$$

$$\phi_2 \le \phi_{1\mathrm{Z}}, \quad \text{where } \phi_2 \ge \phi_{2\mathrm{M}} \text{ is the solution of } A_{\mathrm{E}} j_2(\phi_2) = S_{\mathrm{F}}. \quad \text{(FIIIb)}$$

We note that (FIIIa) implies $q_2 > 0$.

(d) $\phi_1 \in [\phi_{1\mathrm{Z}}, 1]$, $\phi_2 \in [0, \phi_2^{\mathrm{M}}]$ and the decreasing part of $\check{g}_{\mathrm{L}}$ intersects the increasing part of $\hat{g}_{\mathrm{R}}$ at $\phi_1 = \phi_2 = \phi_{1,2}^{\mathrm{int}}$; see Fig. 3(d). This occurs precisely when

$$\phi_{1\mathrm{Z}} \le \phi_{1,2}^{\mathrm{int}} \le \phi_2^{\mathrm{M}}. \quad \text{(FIV)}$$

(e) $\phi_1 \in [\phi_{1\mathrm{Z}}, 1]$, $\phi_2 \in [\phi_2^{\mathrm{M}}, \phi_{2\mathrm{M}}]$ and the decreasing part of $\check{g}_{\mathrm{L}}$ intersects the plateau of $\hat{g}_{\mathrm{R}}$; see Fig. 3(e). Necessary conditions are (FJC) and

$$\phi_{2\mathrm{l}} \le \phi_1 \le \phi_{2\mathrm{r}}, \quad \text{(FV)}$$

where $\phi_{2\mathrm{l}}$ and $\phi_{2\mathrm{r}}$ are the left and right end points of the plateau of $\hat{g}_{\mathrm{R}}$, i.e., $\phi_{2\mathrm{l}}$ is the leftmost and $\phi_{2\mathrm{r}}$ the rightmost (if it exists) solutions of $A_{\mathrm{E}} j_2(\phi) = \eta$, where η is given by (3.8).

(f) $\phi_1 \in [\phi_{1\mathrm{Z}}, 1]$, $\phi_2 \in [\phi_{2\mathrm{M}}, 1]$ and the decreasing part of $\check{g}_{\mathrm{L}}$ intersects the rightmost increasing part of $\hat{g}_{\mathrm{R}}$; see Fig. 3(f). The coupling satisfies $\phi_1 = \phi_2 = \phi_{1,2}^{\mathrm{int}}$.

The case $q_2 < 0$ (which is equivalent to $Q_{\mathrm{F}} < Q_{\mathrm{U}}$) means that $A_{\mathrm{E}} j_2(\cdot)$ is unimodal and has its global minimum at $\phi_{2\mathrm{M}} = 1$. Then, subcases (c) and (f) may occur only if $\phi_1 = \phi_2 = \phi_{1,2}^{\mathrm{int}} = 1$. Then (3.7) implies that also $\phi_{\mathrm{F}} = 1$, which is already removed with our assumption that $0 < \phi_{\mathrm{F}} < 1$. The cases (a), (b), (d) and (e) are on the other hand qualitatively the same irrespective of the sign of q_2.

3.3. *Couplings at $z = z_{\mathrm{W}}$*

Near $z = z_{\mathrm{W}}$ there is no source term of (3.1). The auxiliary functions involved in the entropy condition are $A_{\mathrm{E}} \check{j}_2(\cdot; \phi_2)$ and $A_{\mathrm{E}} \hat{j}_3(\cdot; \phi_3)$. The jump condition

$$j_2(\phi_2) = j_3(\phi_3) \quad \text{(WJC)}$$

is always valid. This case was analysed in Section 3.6 of Ref. 8, from which we extract the following possible couplings considering also (3.2):

(a) $\phi_2 \in [0, \phi_2^{\mathrm{M}}]$, $\phi_3 \in [0, \phi_{3\mathrm{m}}]$. Then $\phi_2 \ge \phi_3$.

(b) $\phi_2 \in [\phi_{2\mathrm{m}}, \phi_{2\mathrm{M}}]$, $\phi_3 = \phi_{3\mathrm{M}}$. The jump condition $j_2(\phi_2) = j_3(\phi_{3\mathrm{M}})$ is satisfied by two values of ϕ_2 in the given interval. Both satisfy $\phi_2 \le \phi_3$. A necessary condition for this coupling is

$$j_2(\phi_2^{\mathrm{M}}) \ge j_3(\phi_{3\mathrm{M}}). \quad \text{(WI)}$$

Table 1. Each row shows a possible entropy-satisfying steady-state solution for the aggregate volume fraction when it is constant in each zone and when the conditions stated are satisfied. The conditions for a coupling between two zones are given and topmost the jump conditions (FJC) and (WJC). The outlet concentrations are given by the explicit formulas (3.3).

	ϕ_1	(FJC)	ϕ_2	(WJC)	ϕ_3
1	0	(FIa), (FIb)	$[0, \phi_2^{\mathrm{M}}]$		$[0, \phi_{3\mathrm{m}}]$
2	0	(FIa), (FIb)	$[\phi_{2\mathrm{m}}, \phi_2^{\mathrm{M}}]$	(WI)	$\phi_{3\mathrm{M}}$
3	0	(FIa), (FIIa), (FIIb)	$[\phi_2^{\mathrm{M}}, \phi_{2\mathrm{M}}]$	(WI)	$\phi_{3\mathrm{M}}$
4	0	(FIIa), (FIIIa), (FIIIb), $q_2 > 0$	$[\phi_{2\mathrm{M}}, 1]$	(WII)	$[\phi_{3\mathrm{M}}, 1]$
5	$[\phi_{1\mathrm{Z}}, 1]$	(FIV)	$[0, \phi_2^{\mathrm{M}}]$		$[0, \phi_{3\mathrm{m}}]$
6	$[\phi_{1\mathrm{Z}}, 1]$	(FIV)	$[\phi_{2\mathrm{m}}, \phi_2^{\mathrm{M}}]$	(WI)	$\phi_{3\mathrm{M}}$
7	$[\phi_{1\mathrm{Z}}, 1]$	(FV)	$[\phi_2^{\mathrm{M}}, \phi_{2\mathrm{M}}]$	(WI)	$\phi_{3\mathrm{M}}$
8	$[\phi_{1\mathrm{Z}}, 1]$	$\phi_1 = \phi_2 = \phi_{1,2}^{\mathrm{int}}$	$[\phi_{2\mathrm{M}}, 1]$	(WII)	$[\phi_{3\mathrm{M}}, 1]$

(c) $\phi_2 \in [\phi_{2\mathrm{M}}, 1]$, $\phi_3 \in [\phi_{3\mathrm{M}}, 1]$. Then $\phi_2 \geq \phi_3$ and a necessary condition is

$$j_2(1) \geq j_3(\phi_{3\mathrm{M}}), \tag{WII}$$

which implies $q_2 \geq 0$.

3.4. *Summary of steady states for the aggregate phase*

The possible combinations of couplings for the three zones inside the column imply the steady states of the aggregate phase shown in Table 1.

Steady-state solutions with a discontinuity inside a zone can be constructed such that the flux values on both sides of the discontinuity are equal; cf. (2.17). Then the discontinuity is stationary and it can be located anywhere in the zone. The jump should also satisfy the entropy condition (2.18). Let $\phi_i^{\downarrow}$ and $\phi_i^{\uparrow}$ denote the solution values below and above a discontinuity, respectively, in zone i. The values to choose from are given in Table 1. The following jumps satisfy the entropy condition (2.18):

$$\begin{aligned}
&\text{zone 3:} \quad \phi_3^{\downarrow} = \phi_{3\mathrm{m}}, && \phi_3^{\uparrow} = \phi_{3\mathrm{M}}, \\
&\text{zone 2:} \quad \phi_2^{\downarrow} \in [\phi_{2\mathrm{m}}, \phi_2^{\mathrm{M}}], && \phi_2^{\uparrow} \in [\phi_2^{\mathrm{M}}, \phi_{2\mathrm{M}}], \quad \text{or} \\
&\qquad\quad\ \ \phi_2^{\downarrow} \in [\phi_{2\mathrm{M}}, 1], && \phi_2^{\uparrow} \in [\phi_2^{\mathrm{M}}, \phi_{2\mathrm{M}}], \\
&\text{zone 1:} \quad \phi_1^{\downarrow} = 0, && \phi_1^{\uparrow} = \phi_{1\mathrm{Z}}.
\end{aligned}$$

3.5. *Desired aggregate steady states*

A steady-state solution is called *desired* if $\phi_{\mathrm{U}} = 0$ and $\phi_3 \geq \phi_{3\mathrm{M}}$, i.e., no aggregates leave through the bottom and there is a layer of froth at the top of the column. Discontinuities can be located in zones 1 and 3; however, such are easily lost from a steady-state situation if any bulk flow changes slightly. We limit the discussion of possible steady states to those that are constant in zones 1 and 3. Table 1 and the

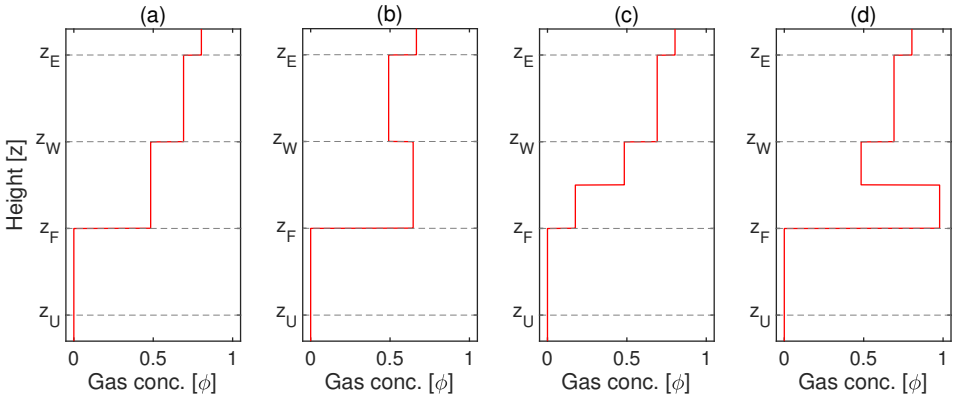

Fig. 4. Desired aggregate steady states $\phi_{\mathrm{SS}i}$, $i = 1, \ldots, 4$, given by (3.9)–(3.11), where values of the bulk velocities are the same as in Fig. 3: $Q_{\mathrm{W}} = 28.0109\,\mathrm{cm}^3/\mathrm{s}$ for ϕ_{SS1}, ϕ_{SS3}, ϕ_{SS4}, and $Q_{\mathrm{W}} = 1.0575\,\mathrm{cm}^3/\mathrm{s}$ for ϕ_{SS2}. All four steady states are physically relevant entropy-satisfying solutions of the PDE (3.1), although ϕ_{SS2} and ϕ_{SS4} are non-monotone.

above-mentioned possible discontinuities within the zones sort out four practically interesting solutions, namely combinations of rows 2, 3 and 4 in Table 1. All four satisfy $\phi_1 = \phi_{\mathrm{U}} = 0$, $\phi_{\mathrm{E}} = A_{\mathrm{E}} j_3(\phi_3)/Q_{\mathrm{E}} \geq \phi_{3\mathrm{M}}$ and the jump condition (FJC) and (WJC). The first steady state is constant in each zone:

$$\phi_{\mathrm{SS1}}(z) := \begin{cases} \phi_3 = \phi_{3\mathrm{M}} \geq \phi_2 & \text{for } z_{\mathrm{W}} \leq z < z_{\mathrm{E}}, \\ \phi_2 \in [\phi_{2\mathrm{m}}, \phi_{2\mathrm{M}}] & \text{for } z_{\mathrm{F}} \leq z < z_{\mathrm{W}}, \\ 0 & \text{for } z < z_{\mathrm{F}}, \end{cases} \tag{3.9}$$

and necessary conditions are (WI) and either (FIa)–(FIb) if $\phi_2 \in [\phi_{2\mathrm{m}}, \phi_2^{\mathrm{M}}]$, or (FIa), (FIIa)–(FIIb) if $\phi_2 \in [\phi_2^{\mathrm{M}}, \phi_{2\mathrm{M}}]$. The second is also constant in each zone:

$$\phi_{\mathrm{SS2}}(z) := \begin{cases} \phi_3 \in [\phi_{3\mathrm{M}}, 1] & \text{for } z_{\mathrm{W}} \leq z < z_{\mathrm{E}}, \\ \phi_2 \in [\phi_{2\mathrm{M}}, 1] & \text{for } z_{\mathrm{F}} \leq z < z_{\mathrm{W}}, \\ 0 & \text{for } z < z_{\mathrm{F}}, \end{cases} \tag{3.10}$$

where $\phi_2 \geq \phi_3$, and necessary conditions are (FIIa), (FIIIa)–(FIIIb) and (WII); hence $q_2 > 0$. The remaining solutions have a discontinuity located at z_{d} anywhere in zone 2:

$$\phi_{\mathrm{SS3}}(z) := \begin{cases} \phi_3 = \phi_{3\mathrm{M}} & \text{for } z_{\mathrm{W}} \leq z < z_{\mathrm{E}}, \\ \phi_2^{\uparrow} \in [\phi_2^{\mathrm{M}}, \phi_{2\mathrm{M}}] & \text{for } z_{\mathrm{d}} \leq z < z_{\mathrm{W}}, \\ \phi_2^{\downarrow} \in [\phi_{2\mathrm{m}}, \phi_2^{\mathrm{M}}] & \text{for } z_{\mathrm{F}} \leq z < z_{\mathrm{d}}, \\ 0 & \text{for } z < z_{\mathrm{F}}. \end{cases}$$

This solution is non-decreasing with z and the necessary conditions are (FIa), (FIIa)–(FIIb) and (WI). In condition (FIIb), $\phi_2 = \phi_2^{\uparrow}$ should be used. Then (FIb)

is implied by (FIIb) (where $\phi_2 = \phi_2^{\downarrow}$ is used), since $\phi_2^{\downarrow} \le \phi_2^{\uparrow}$. The fourth solution, which is non-monotone (if $Q_{\mathrm{W}} > 0$), is

$$\phi_{\mathrm{SS4}}(z) := \begin{cases} \phi_3 = \phi_{3\mathrm{M}} & \text{for } z_{\mathrm{W}} \le z < z_{\mathrm{E}}, \\ \phi_2^{\uparrow} \in [\phi_2^{\mathrm{M}}, \phi_{2\mathrm{M}}] & \text{for } z_{\mathrm{d}} \le z < z_{\mathrm{W}}, \\ \phi_2^{\downarrow} \in [\phi_{2\mathrm{M}}, 1] & \text{for } z_{\mathrm{F}} \le z < z_{\mathrm{d}}, \\ 0 & \text{for } z < z_{\mathrm{F}}, \end{cases} \tag{3.11}$$

which requires (FIa), (FIIa)–(FIIb), (FIIIa)–(FIIIb) and (WI). This solution will be discarded later as an undesired solution when imposing conditions on the use of wash water; see Section 5.

4. Construction of steady states for the solid phase

We now assume that a steady-state solution of (3.1), i.e. the first equation of (1.1), is a known piecewise constant function and seek steady-state solutions $\varphi = \varphi(z)$ of the second equation of (1.1). We do this for the four desired steady-state solutions $\phi_{\mathrm{SS}k}$, $k = 1, \dots, 4$, given each solution of the aggregate phases (3.9)–(3.11). Then the second equation of (1.1) becomes

$$\frac{\partial}{\partial t}\big(A(z)(1-\phi_{\mathrm{SS}k}(z))\varphi\big) - \frac{\partial}{\partial z}\big(A(z)F(\varphi, \phi_{\mathrm{SS}k}(z), z, t)\big) = Q_{\mathrm{F}}(t)\phi_{\mathrm{s,F}}(t)\delta_{z_{\mathrm{F}}}. \tag{4.1}$$

(The t-variable is suppressed from now on.) The possible couplings across the spatial discontinuities of the flux functions $A(\cdot)F(\varphi, \phi_{\mathrm{SS}k}(\cdot), \cdot)$, $k = 1, \dots, 4$, will now be investigated. The possible sedimentation flux functions are

$$\begin{aligned} f_3(\varphi, \phi_3) &= (1-\phi_3)f_{\mathrm{b}}(\varphi) + \big(j_{\mathrm{b}}(\phi_3) - (1-\phi_3)q_3\big)\varphi && \text{for } z_{\mathrm{W}} < z < z_{\mathrm{E}}, \\ f_2(\varphi, \phi_2^{\uparrow}) &= (1-\phi_2^{\uparrow})f_{\mathrm{b}}(\varphi) + \big(j_{\mathrm{b}}(\phi_2^{\uparrow}) - (1-\phi_2^{\uparrow})q_2\big)\varphi && \text{for } z_{\mathrm{d}} < z < z_{\mathrm{W}}, \\ f_2(\varphi, \phi_2^{\downarrow}) &= (1-\phi_2^{\downarrow})f_{\mathrm{b}}(\varphi) + \big(j_{\mathrm{b}}(\phi_2^{\downarrow}) - (1-\phi_2^{\downarrow})q_2\big)\varphi && \text{for } z_{\mathrm{F}} < z < z_{\mathrm{d}}, \\ f_1(\varphi, 0) &= f_{\mathrm{b}}(\varphi) - q_1\varphi && \text{for } z_{\mathrm{U}} < z < z_{\mathrm{F}}, \end{aligned}$$

with obvious modification for $\phi_{\mathrm{SS}1}$ and $\phi_{\mathrm{SS}2}$ which have no discontinuity in zone 2.

We recall that the total flux F and the zone fluxes f_k are positive in the direction of sedimentation, i.e. opposite to the direction of the z-axis. One could formally perform the variable change $\xi := -z$ in (4.1); however, instead we keep in mind that in this section the auxiliary functions $\check{g}_{\mathrm{L}}$ and $\hat{g}_{\mathrm{R}}$ in the entropy condition (2.19) are considered to be positive in the downward ξ-direction, so that $\check{g}_{\mathrm{L}}$ and $\hat{g}_{\mathrm{R}}$ refer to the local fluxes above and below, respectively, a given spatial discontinuity.

4.1. *Couplings at $z = z_{\mathrm{U}}$ and $z = z_{\mathrm{E}}$*

In each of the four cases of $\phi_{\mathrm{SS}k}$, the flux function $A(z)F(\varphi, \phi, z)$ in (4.1) becomes the following on either side of the underflow location $z = z_{\mathrm{U}}$, with $\phi_1 = \phi_{\mathrm{U}} = 0$,

$$g_{\mathrm{L}}(\varphi) = A_{\mathrm{U}} f_1(\varphi, 0) = A_{\mathrm{U}} f_{\mathrm{b}}(\varphi) + Q_{\mathrm{U}}\varphi, \quad z > z_{\mathrm{U}},$$

$$g_{\mathrm{R}}(\varphi) = A_{\mathrm{U}} f_{\mathrm{U}}(\varphi, 0) = Q_{\mathrm{U}}\varphi, \qquad z < z_{\mathrm{U}}.$$

This is the normal case at the underflow of a clarifier-thickener and the possible entropy-satisfying steady-state solutions satisfy (see Section 9 in Ref. 18; cf. Section 3.1):

$$\varphi_1 \in [0, \varphi_{1\mathrm{m}}] \cup [\varphi_{1\mathrm{M}}, 1], \qquad \varphi_{\mathrm{U}} = \varphi_1 + \frac{A_{\mathrm{U}}}{Q_{\mathrm{U}}} f_{\mathrm{b}}(\varphi_1) \in [0, 1], \tag{4.2}$$

where the values $\varphi_{1\mathrm{m}}$ and $\varphi_{1\mathrm{M}}$ refer to the function $f_1(\cdot, 0)$ (see Section 2.6).

The two flux functions on either side of $z = z_{\mathrm{E}}$ are

$$\begin{aligned}
g_{\mathrm{L}}(\varphi) &= A_{\mathrm{E}} f_{\mathrm{E}}(\varphi, \phi_{\mathrm{E}}) = -(1-\phi_{\mathrm{E}}) Q_{\mathrm{E}}\varphi && \text{for } z > z_{\mathrm{E}},\\
g_{\mathrm{R}}(\varphi) &= A_{\mathrm{E}} f_3(\varphi, \phi_3)\\
&= A_{\mathrm{E}}(1-\phi_3) f_{\mathrm{b}}(\varphi) + \big(A_{\mathrm{E}} j_{\mathrm{b}}(\phi_3) - (1-\phi_3) Q_3\big)\varphi\\
&= A_{\mathrm{E}}(1-\phi_3) f_{\mathrm{b}}(\varphi) + \big(A_{\mathrm{E}} j_3(\phi_3) - Q_3\big)\varphi,\\
&= A_{\mathrm{E}}(1-\phi_3) f_{\mathrm{b}}(\varphi) - (1-\phi_{\mathrm{E}}) Q_{\mathrm{E}}\varphi && \text{for } z < z_{\mathrm{E}},
\end{aligned}$$

where the last equality follows from (3.3). Irrespective of $\phi_{\mathrm{SS}k}$, $k = 1, 2, 3$, the situation is analogous to the effluent level of a clarifier-thickener and the entropy-satisfying steady-state solutions satisfy (see Section 9 in Ref. 18; cf. Section 3.1):

$$\varphi_3 \in \{0\} \cup [\varphi_{3\mathrm{Z}}, 1], \qquad \varphi_{\mathrm{E}} = -\frac{A_{\mathrm{E}} f_3(\varphi_3, \phi_3)}{(1-\phi_{\mathrm{E}}) Q_{\mathrm{E}}} \in [0, 1], \tag{4.3}$$

where $\varphi_{3\mathrm{Z}}$ is the positive zero of $f_3(\cdot, \phi_3)$.

4.2. *Couplings at $z = z_{\mathrm{W}}$*

Near $z = z_{\mathrm{W}}$, there is no source term in (4.1). The flux functions on either side can be written as follows, where ϕ_2 should be replaced by $\phi_2^{\uparrow}$ in the case of $\phi_{\mathrm{SS}3}$ or $\phi_{\mathrm{SS}4}$:

$$\begin{aligned}
g_{\mathrm{L}}(\varphi) &= A_{\mathrm{E}} f_3(\varphi, \phi_3) = A_{\mathrm{E}}(1-\phi_3) f_{\mathrm{b}}(\varphi) + \big(A_{\mathrm{E}} j_3(\phi_3) - Q_{\mathrm{E}}\big)\varphi && \text{for } z > z_{\mathrm{W}},\\
g_{\mathrm{R}}(\varphi) &= A_{\mathrm{E}} f_2(\varphi, \phi_2) = A_{\mathrm{E}}(1-\phi_2) f_{\mathrm{b}}(\varphi) + \big(A_{\mathrm{E}} j_2(\phi_2) - Q_{\mathrm{E}} + Q_{\mathrm{W}}\big)\varphi && \text{for } z < z_{\mathrm{W}},
\end{aligned}$$

The jump condition is

$$f_2(\varphi_2, \phi_2) = f_3(\varphi_3, \phi_3) \tag{WJCs}$$

Since $\phi_{\mathrm{U}} = 0$ for the desired steady states, the conservation law implies $Q_{\mathrm{F}}\phi_{\mathrm{F}} = A_{\mathrm{E}} j_2(\phi_2) = A_{\mathrm{E}} j_3(\phi_3) = Q_{\mathrm{E}}\phi_{\mathrm{E}}$. Hence, we can rewrite the flux functions as

$$\begin{aligned}
g_{\mathrm{L}}(\varphi) &= A_{\mathrm{E}}(1-\phi_3) f_{\mathrm{b}}(\varphi) - Q_{\mathrm{E}}(1-\phi_{\mathrm{E}})\varphi && \text{for } z > z_{\mathrm{W}},\\
g_{\mathrm{R}}(\varphi) &= A_{\mathrm{E}}(1-\phi_2) f_{\mathrm{b}}(\varphi) + \big(-Q_{\mathrm{E}}(1-\phi_{\mathrm{E}}) + Q_{\mathrm{W}}\big)\varphi\\
&= A_{\mathrm{E}}(1-\phi_2) f_{\mathrm{b}}(\varphi) + \big(Q_{\mathrm{F}}\phi_{\mathrm{F}} + Q_{\mathrm{U}} - Q_{\mathrm{F}}\big)\varphi && \text{for } z < z_{\mathrm{W}}.
\end{aligned}$$

We have $g_{\mathrm{L}}(0) = g_{\mathrm{R}}(0) = 0$, $g_{\mathrm{L}}(1) = -Q_{\mathrm{E}}(1-\phi_{\mathrm{E}}) \le 0$ and $g_{\mathrm{R}}(1) - g_{\mathrm{L}}(1) = Q_{\mathrm{W}} \ge 0$. Hence, g_{L} is unimodal and has the two zeros 0 and $\varphi_{3\mathrm{Z}}$. The larger $Q_{\mathrm{E}}(1-\phi_{\mathrm{E}})$ is, the closer $\varphi_{3\mathrm{Z}}$ is to zero, and below a certain value, g_{L} is decreasing with only

$\varphi_{3\mathrm{Z}} = 0$ as its zero. The analogous situation holds for g_R and $\varphi_{2\mathrm{Z}}$. The latter value does not exist if g_R is decreasing; hence, we impose

$$\frac{\partial g_\mathrm{R}}{\partial \varphi}(0,\phi_2) > 0 \quad \Leftrightarrow \quad Q_\mathrm{U} - Q_\mathrm{F}(1-\phi_\mathrm{F}) > -A_\mathrm{E}(1-\phi_2)u_\mathrm{sf}^\infty. \tag{WIs}$$

If (WIs) holds, then the existence of $\varphi_{2\mathrm{Z}}$ depends on the sign of $g_\mathrm{R}(1) = Q_\mathrm{U} - Q_\mathrm{F}(1-\phi_\mathrm{F})$. This leads to the complementary conditions $g_\mathrm{R}(1) \le 0$, which is (FIIIa), and

$$Q_\mathrm{U} > Q_\mathrm{F}(1-\phi_\mathrm{F}). \tag{$\complement$FIIIa}$$

Combining these conditions with the possible steady-state values of φ_3 given by (4.3), we have the following cases:

(a) $\varphi_3 = 0$, (WIs) and (FIIIa). The possible couplings are $\varphi_2 = 0$ and $\varphi_2 = \varphi_{2\mathrm{Z}}$, where $\varphi_{2\mathrm{Z}}$ is the positive zero of $f_2(\cdot,\phi_2)$; see Fig. 5(a1) and (a2).
(b) $\varphi_3 \in [\varphi_{3\mathrm{Z}}, 1]$, (WIs) and (FIIIa). The only possibility is $\varphi_2 \in [\varphi_{2\mathrm{Z}}, 1]$; see Fig. 5(b).
(c) $\varphi_3 = 0$ and ($\complement$FIIIa). The only solution is $\varphi_2 = 0$; see Fig. 5(c).
(d) $\varphi_3 \in [\varphi_{3\mathrm{Z}}, 1]$ and ($\complement$FIIIa). This case is empty, since $\check{g}_\mathrm{L}(\cdot;\varphi_3)$ with $\varphi_3 \ge \varphi_{3\mathrm{Z}}$ will necessarily intersect $\hat{g}_\mathrm{R}$ at a positive flux value, while $g_\mathrm{L}(\varphi_3) < 0$.

In conclusion, the following values are so far candidates in zone 2:

$$\varphi_2 \in \{0\} \cup [\varphi_{2\mathrm{Z}}, 1]. \tag{4.4}$$

4.3. *Couplings at $z = z_\mathrm{F}$*

Consider Equation (4.1) near $z = z_\mathrm{F}$. We set $S_{\mathrm{s,F}} := \phi_{\mathrm{s,F}} Q_\mathrm{F}$ and move the source term into the total flux function with the identity

$$S_{\mathrm{s,F}}\delta_{z_\mathrm{F}} = S_{\mathrm{s,F}} \frac{\mathrm{d}}{\mathrm{d}z} H_{z_\mathrm{F}}.$$

Hence, the term $S_{\mathrm{s,F}}$ should be subtracted from the flux in zone 2 counted in the z-direction. In the downwards ξ-direction, the fluxes above and below the discontinuity, denoted by g_L and g_R, respectively, are given by the following (where we have used that $Q_\mathrm{F}\phi_\mathrm{F} = A_\mathrm{E} j_2(\phi_2)$ and $Q_2 = -Q_\mathrm{U} + Q_\mathrm{F}$)

$$\begin{aligned} g_\mathrm{L}(\varphi) &= A_\mathrm{E} f_2(\varphi,\phi_2) + S_{\mathrm{s,F}} \\ &= A_\mathrm{E}(1-\phi_2) f_\mathrm{b}(\varphi) + \big(A_\mathrm{E} j_\mathrm{b}(\phi_2) - (1-\phi_2)Q_2\big)\varphi + S_{\mathrm{s,F}} \\ &= A_\mathrm{E}(1-\phi_2) f_\mathrm{b}(\varphi) + \big(A_\mathrm{E} j_2(\phi_2) - Q_2\big)\varphi + S_{\mathrm{s,F}} \\ &= A_\mathrm{E}(1-\phi_2) f_\mathrm{b}(\varphi) + \big(Q_\mathrm{F}\phi_\mathrm{F} + Q_\mathrm{U} - Q_\mathrm{F}\big)\varphi + S_{\mathrm{s,F}} \\ &= A_\mathrm{E}(1-\phi_2) f_\mathrm{b}(\varphi) + \big(Q_\mathrm{U} - Q_\mathrm{F}(1-\phi_\mathrm{F})\big)\varphi + S_{\mathrm{s,F}} \qquad \text{for } z > z_\mathrm{F}, \end{aligned} \tag{4.5}$$

$$g_\mathrm{R}(\varphi) = A_\mathrm{U} f_1(\varphi,0) = A_\mathrm{U} f_\mathrm{b}(\varphi) + Q_\mathrm{U}\varphi \qquad \text{for } z < z_\mathrm{F}. \tag{4.6}$$

In the cases $\phi_{\mathrm{SS}3}$ and $\phi_{\mathrm{SS}4}$, ϕ_2 should be replaced by $\phi_2^\downarrow$. The jump condition is

$$A_\mathrm{U} f_1(\varphi_1,0) = A_\mathrm{E} f_2(\varphi_2,\phi_2) + S_{\mathrm{s,F}}. \tag{FJCs}$$

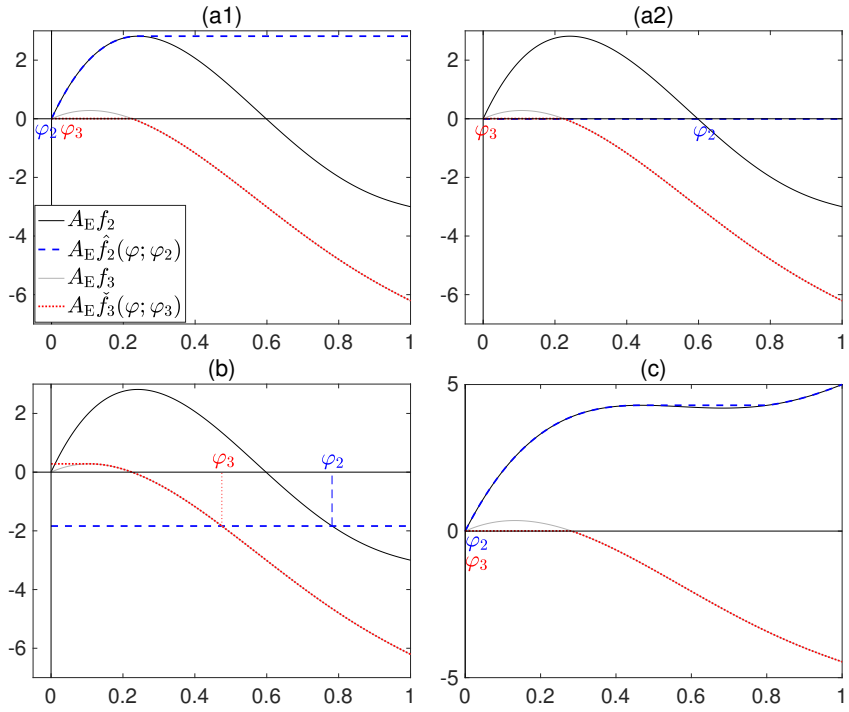

Fig. 5. Couplings at $z = z_W$ for the solids PDE for (a1), (a2), (b) $Q_U = 13\,\mathrm{cm}^3/\mathrm{s}$, $Q_F = 40\,\mathrm{cm}^3/\mathrm{s}$ and $Q_W = 3.21\,\mathrm{cm}^3/\mathrm{s}$, satisfying (FIIIa), (c) $Q_U = 25\,\mathrm{cm}^3/\mathrm{s}$, $Q_F = 40\,\mathrm{cm}^3/\mathrm{s}$ and $Q_W = 9.46\,\mathrm{cm}^3/\mathrm{s}$, satisfying (CFIIIa). All cases are computed using a steady state of type ϕ_{SS1} for ϕ. Note that these flux functions depend on the solution ϕ_{SS1}; see (2.12). For example, the slopes of the linear term of the flux functions $A_E f_2$ and $A_E f_3$ in plots (a1)–(b) are $A_E j_2(\phi_{SS1,2}) - Q_2 \approx -3.0\,\mathrm{cm}^3/\mathrm{s}$ and $A_E j_3(\phi_{SS1,3}) - Q_3 \approx -6.21\,\mathrm{cm}^3/\mathrm{s}$.

Lemma 4.1. *The continuous functions g_L and g_R given by* (4.5) *and* (4.6) *intersect in one, two or three points $\varphi_{1,2}^{\mathrm{int}} \in (0,1)$ satisfying*

$$\big(A_U - A_E(1-\phi_2)\big) f_b(\varphi_{1,2}^{\mathrm{int}}) + (1-\phi_F) Q_F \varphi_{1,2}^{\mathrm{int}} - S_{s,F} = 0. \tag{4.7}$$

Furthermore, f_b, g_L and g_R have the same concave-convex form with the same inflection point.

Proof. The left-hand side of (4.7) is the difference of the fluxes (4.6) and (4.5):

$$d(\varphi) := g_R(\varphi) - g_L(\varphi) = \big(A_U - A_E(1-\phi_2)\big) f_b(\varphi) + (1-\phi_F) Q_F \varphi - S_{s,F}.$$

The continuous function d satisfies $d(0) = -S_{s,F} < 0$ and

$$d(1) = (1-\phi_F) Q_F - S_{s,F} = (1 - \phi_F - \phi_{s,F}) Q_F = \phi_{f,F} Q_F > 0.$$

Moreover, d, f_b, g_L and g_R have the same concave-convex form with the same inflection point, since

$$d''(\varphi) = g_\mathrm{L}''(\varphi) - g_\mathrm{R}''(\varphi) = (A_\mathrm{U} - A_\mathrm{E}(1-\phi_2))f_\mathrm{b}''(\varphi). \qquad \square$$

The task is now to couple φ_2 and φ_1 given by (4.4) and (4.2), respectively:

(a) $\varphi_2 = 0$, $\varphi_1 \in [0, \varphi_{1\mathrm{m}}]$; see Fig. 6(a). The value $\varphi_1 \le \varphi_{1\mathrm{m}}$ is the unique solution of $g_\mathrm{R}(\varphi_1) = S_{\mathrm{s,F}}$ according to (FJCs). This coupling is possible only if

$$g_\mathrm{R}(\varphi_{1\mathrm{m}}) = g_\mathrm{R}(\varphi_{1\mathrm{M}}) \ge S_{\mathrm{s,F}} \quad \Leftrightarrow \quad A_\mathrm{U} f_1(\varphi_{1\mathrm{M}}, 0) \ge S_{\mathrm{s,F}}. \tag{FIas}$$

(b) $\varphi_2 = 0$, $\varphi_1 \in [\varphi_{1\mathrm{M}}, 1]$; see Fig. 6(b). The value $\varphi_1 \ge \varphi_{1\mathrm{M}}$ is the unique solution of $g_\mathrm{R}(\varphi_1) = S_{\mathrm{s,F}}$ according to (FJCs). This coupling is possible only if

$$A_\mathrm{U} f_1(\varphi_{1\mathrm{M}}, 0) \le S_{\mathrm{s,F}}, \tag{CFIas}$$

$$A_\mathrm{U} f_1(1, 0) \ge S_{\mathrm{s,F}} \quad \Leftrightarrow \quad Q_\mathrm{U} \ge S_{\mathrm{s,F}}. \tag{FIbs}$$

There are two subcases depending on whether g_L is unimodal or not:

- $g_\mathrm{L}(1) > S_{\mathrm{s,F}} \Leftrightarrow$ (CFIIIa); see Fig. 6(b1): The solution exists without further restrictions.
- $g_\mathrm{L}(1) \le S_{\mathrm{s,F}} \Leftrightarrow$ (FIIIa); see Fig. 6(b2): A coupling is possible only if also (WIs) and the following conditions hold:

$$A_\mathrm{U} f_1(\varphi_{2\mathrm{Z}}, 0) \ge S_{\mathrm{s,F}}, \tag{FIIs}$$

$$\varphi_{1\mathrm{M}} \le \varphi_{2\mathrm{Z}}. \tag{FIIIs}$$

(c) $\varphi_2 \in [\varphi_{2\mathrm{Z}}, 1]$, $\varphi_1 \in [0, \varphi_{1\mathrm{m}}]$; see Fig. 6(c). The decreasing part of $\check{g}_\mathrm{L}$ intersects the first increasing part of $\hat{g}_\mathrm{R}$. Necessarily, (WIs) and (FIIIa) hold. The coupling satisfies $\varphi_1 = \varphi_2 = \varphi_{1,2}^{\mathrm{int}}$, which is the unique solution of (4.7) satisfying

$$\varphi_{2\mathrm{Z}} \le \varphi_{1,2}^{\mathrm{int}} \le \varphi_{1\mathrm{m}}. \tag{FIVs}$$

(d) $\varphi_2 \in [\varphi_{2\mathrm{Z}}, 1]$, $\varphi_1 \in [\varphi_{1\mathrm{M}}, 1]$; see Fig. 6(d). Necessarily, (WIs) and (FIIIa) hold. The decreasing part of $\check{g}_\mathrm{L}$ intersects the rightmost increasing part of $\hat{g}_\mathrm{R}$. The coupling satisfies $\varphi_1 = \varphi_2 = \varphi_{1,2}^{\mathrm{int}}$, which is the unique solution of (4.7) greater than $\varphi_{1\mathrm{M}}$.

4.4. *Summary of steady states for the solid phase*

The steady-state solutions $\phi_{\mathrm{SS}1}$ and $\phi_{\mathrm{SS}2}$ are constant in every zone and Table 2 gives the possible steady-state solutions for $\varphi(z)$ that are constant in zones 1, 2 and 3. The outlet concentrations are given by the explicit formulas (4.2)–(4.3).

There may also be a discontinuity of $\varphi(z)$ within any of these zones. As before, we let $\varphi_k^\uparrow$ and $\varphi_k^\downarrow$ denote the solution values above and below a discontinuity, respectively, in zone k. From Table 2, we can conclude that the following jumps, which satisfy the entropy condition (2.18), are possible:

$$\text{zone 3:} \quad \varphi_3^\uparrow = 0, \qquad \varphi_3^\downarrow = \varphi_{3\mathrm{Z}},$$

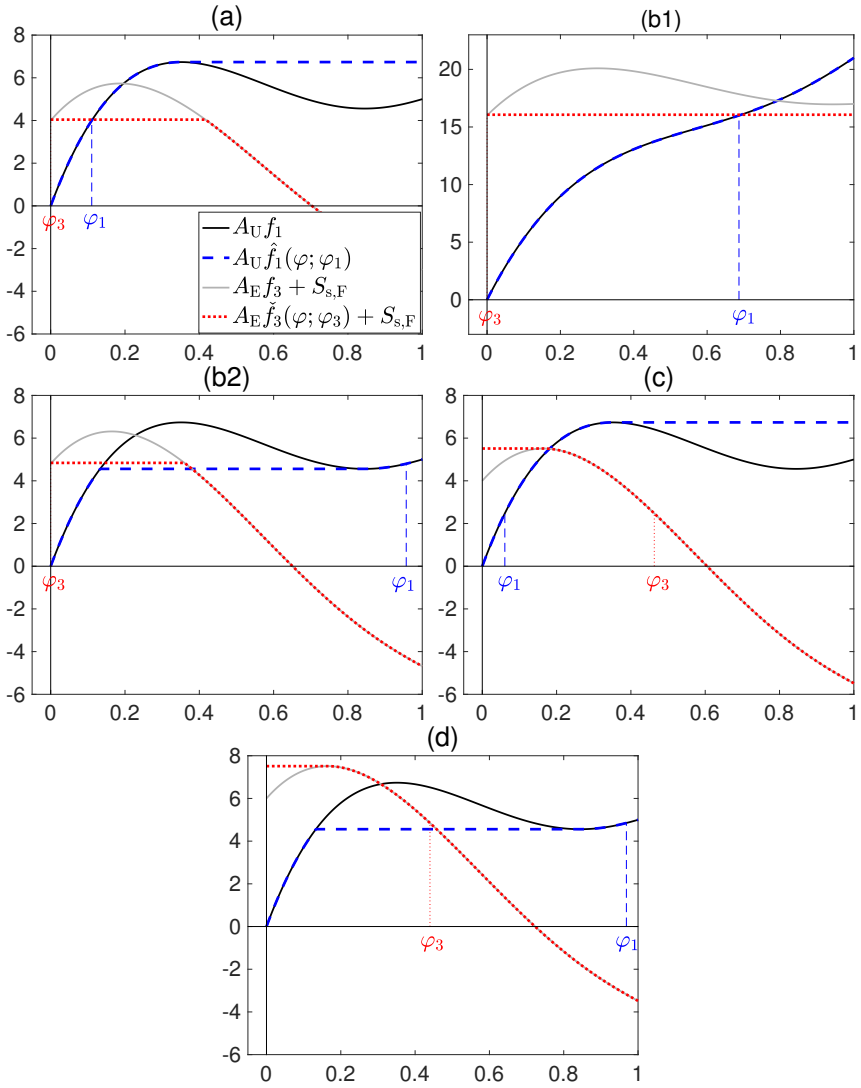

Fig. 6. Couplings at $z = z_F$ for the solids PDE for (a), (c) $Q_U = 5\,\mathrm{cm}^3/\mathrm{s}$, $Q_F = 40\,\mathrm{cm}^3/\mathrm{s}$ and $Q_W = 1.34\,\mathrm{cm}^3/\mathrm{s}$ with $\phi_F = 0.7$ and $\phi_{s,F} = 0.1$, (b1) $Q_U = 21\,\mathrm{cm}^3/\mathrm{s}$, $Q_F = 40\,\mathrm{cm}^3/\mathrm{s}$ and $Q_W = 5.45\,\mathrm{cm}^3/\mathrm{s}$ with $\phi_F = 0.5$ and $\phi_{s,F} = 0.4$, (b2) $\phi_F = 0.7$ and $\phi_{s,F} = 0.12$, (d) $\phi_F = 0.7$ and $\phi_{s,F} = 0.15$. All cases are computed using a steady-state of type ϕ_{SS1} for ϕ.

$$\begin{aligned} &\text{zone 2:} \quad \varphi_2^{\uparrow} = 0, \qquad \varphi_2^{\downarrow} = \varphi_{2Z}, \\ &\text{zone 1:} \quad \varphi_1^{\uparrow} = \varphi_{1m}, \quad \varphi_1^{\downarrow} = \varphi_{1M}. \end{aligned}$$

We next couple the desired steady states of ϕ with the possible ones of φ. In order to reduce the number of steady states, we impose further restrictions on what we

Table 2. Possible entropy-satisfying stationary solutions $\varphi(z)$ having a constant value in each zone inside the flotation column with necessary conditions for each coupling, given any of the solutions ϕ_{SS1} or ϕ_{SS2}, which are constant in each zone. The jump conditions (FJCs) and (WJCs) always hold and are therefore written topmost.

	φ_1	(FJCs)	φ_2	(WJCs)	φ_3
1	$[0, \varphi_{1\mathrm{m}}]$	(FIas)	0		0
2	$[0, \varphi_{1\mathrm{m}}]$	(WIs), (FIIIa), (FIVs)	$[\varphi_{2\mathrm{Z}}, 1]$	(WIs), (FIIIa)	$[\varphi_{3\mathrm{Z}}, 1]$
3	$[\varphi_{1\mathrm{M}}, 1]$	(FIIIa), (CFIas), (FIbs), (WIs), (FIIs), (FIIIs)	0		0
4	$[\varphi_{1\mathrm{M}}, 1]$	(CFIIIa), (CFIas), (FIbs)	0		0
5	$[\varphi_{1\mathrm{M}}, 1]$	(WIs), (FIIIa), $\varphi_1 = \varphi_2$	$\varphi_{2\mathrm{Z}}$	(WIs), (FIIIa)	0
6	$[\varphi_{1\mathrm{M}}, 1]$	(WIs), (FIIIa), $\varphi_1 = \varphi_2$	$[\varphi_{2\mathrm{Z}}, 1]$	(WIs), (FIIIa)	$[\varphi_{3\mathrm{Z}}, 1]$

regard as desired steady states.

One of the purposes of a flotation column is to separate out the hydrophilic solids through the underflow. Consequently, given the possibilities in Table 2, any desired steady state for the solid phase should satisfy $\varphi_{\mathrm{E}} = 0$ and we also require $\varphi_3 = 0$ (although it is mathematically possible to have a discontinuity within zone 3). Row 1 of Table 2 gives one possible desired solution with a low φ_1 and hence a low underflow volume fraction of solids. Rows 3 and 4 mean that either $\varphi_1 \in [\varphi_{1\mathrm{M}}, 1]$ for a constant solution in zone 1 or $\varphi_1^{\downarrow} = \varphi_{1\mathrm{M}}$ for a solution with a discontinuity in zone 1. Moreover, we assume that either $\varphi_2 = 0$ or if there are particles in zone 2, they are not moving upwards, i.e., $f_2(\varphi_2, \phi_2) = 0$. Generally, one wants to avoid high volumetric flows, which rules out solutions that require condition (FIVs).

5. Desired steady states with and without wash water

5.1. *Conditions on the wash water*

We have always assumed that the effluent volume fraction Q_{E} is positive, i.e.

$$Q_{\mathrm{E}} = Q_2 + Q_{\mathrm{W}} = -Q_{\mathrm{U}} + Q_{\mathrm{F}} + Q_{\mathrm{W}} > 0, \tag{E}$$

where the volumetric flow in zone 2 is $Q_2 := -Q_{\mathrm{U}} + Q_{\mathrm{F}}$. Wash water is optional in a flotation column. If $Q_{\mathrm{W}} = 0$, then (E) implies $Q_2 > 0$. Since there is no injection of fluid above the feed inlet, we conclude that the fluid flow (not identical to the bulk flow) in zone 2 must be positive, or at least non-negative.

Now consider the case when wash water is applied, i.e. $Q_{\mathrm{W}} > 0$. Then Q_2 can have any sign and so can the fluid flow in zone 2. Although we do not model explicitly the washing process in the froth region, i.e., hydrophilic particles are washed off the foam, we impose the natural requirement that the fluid flow in zone 2 should be downwards, i.e., negative. In view of (2.5), this gives the following condition:

$$q_2 - \phi_2 v_{\mathrm{a},2} - \phi_{\mathrm{s},2} v_{\mathrm{s},2} < 0. \tag{5.1}$$

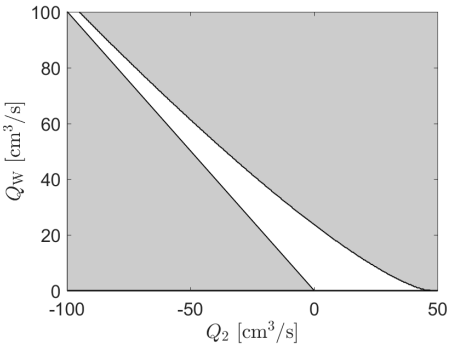

Fig. 7. Operating chart showing the possible interval for Q_W for a given $Q_2 = -Q_U + Q_F$. The lower bound is given by $Q_W \geq 0$ and (E), and the upper bound by condition (WI). The white region of allowed points is bounded with a vertex at $(Q_2, Q_W) = A_E q_{neg}(1,1) \approx (-195.1, 195.1)$ cm^3/s.

This condition can be rewritten in terms of controllable variables and the input volume fraction ϕ_F. Firstly, $q_2 = (-Q_U + Q_F)/A_E$. Secondly, a desired solution has either no solids in zone 2, $\phi_{s,2} = 0$, or we may allow a stationary discontinuity with only fluid above. In both cases, the flux of solids in zone 2 is zero: $\phi_{s,2} v_{s,2} = 0$. Thirdly, all aggregates that are fed to the column passes zone 2 and then rise to the effluent; hence, $Q_F \phi_F = A_E \phi_2 v_{a,2} = A_E j_2(\phi_2)$. Thus, (5.1) can be rewritten as

$$-Q_U + Q_F - Q_F \phi_F < 0,$$

which is in fact precisely condition (CFIIIa). Thus, when $Q_W > 0$, wash water is effective only if (CFIIIa) holds. Consequently, (FIIIa) implies that one can as well choose $Q_W = 0$, since a positive value means that all injected wash water will leave through the effluent.

Of all necessary inequality conditions for the desired steady states ϕ_{SSk}, $k = 1, \ldots, 4$, and those in Table 2 that satisfy $\varphi_3 = 0$, only (WI) involves Q_W. For a given Q_2, (WI) gives an upper bound for Q_W, whereas (E) together with $Q_W \geq 0$ is a lower bound; see Fig. 7. If $Q_2 < 0$, then the wash water condition is satisfied; however, it can be satisfied also for small positive values $Q_2 < Q_F \phi_F$. If the conditions for a steady state are such that one has to choose $Q_2 > 0$, then (E) is satisfied and there is no need to choose a positive value of Q_W. Thus, to have wash water in effect in the froth region in zone 2, one should, if possible, choose values on the volumetric flows so that $Q_2 < 0$, and then choose $Q_W > 0$ so that (E) satisfied.

For the steady states ϕ_{SS2} and ϕ_{SS4} (which require (FIIIa)), we set $Q_W = 0$. When $Q_W = 0$, there is no spatial discontinuity at $z = z_W$, which implies that the only possible entropy-satisfying connection at z_W for ϕ_{SS4} is $\phi_{2M} = \phi_{3M}$, i.e., the solution is continuous. This implies in turn that the entropy-satisfying solution at z_d is continuous and equal to ϕ_{2M}. Thus, in the cases there is no wash water, ϕ_{SS4}

reduces to a special case of ϕ_{SS2}, given by (3.10), namely

$$\phi_{\mathrm{SS20}} = \begin{cases} \phi_2 = \phi_3 = \phi_{2\mathrm{M}} & \text{for } z_{\mathrm{F}} \le z < z_{\mathrm{E}}, \\ 0 & \text{for } z < z_{\mathrm{F}}. \end{cases}$$

Consequently, only the solutions ϕ_{SS1} and ϕ_{SS3} allow working wash water. Since wash water is an advantage, we require condition (CFIIIa) to hold for these cases.

In conclusion, we have the following division of desired steady states with and without wash water:

$$\phi_{\mathrm{SS1}} \text{ and } \phi_{\mathrm{SS3}} \text{ require (CFIIIa) and } Q_{\mathrm{W}} > 0, \tag{WW}$$

$$\phi_{\mathrm{SS2}} \text{ and the special case } \phi_{\mathrm{SS20}} \text{ require (FIIIa) and } Q_{\mathrm{W}} = 0. \tag{CWW}$$

We now couple these solutions with the desired steady states for φ. The steady states for the solids volume fraction are then given through $\phi_{\mathrm{s}}^{\mathrm{SS}k\ell} = (1 - \phi_{\mathrm{SS}k})\varphi_{\mathrm{SS}\ell}$.

5.2. *Steady states of the solid phase in the case* ϕ_{SS1}

According to (WW), we require (CFIIIa) for ϕ_{SS1}. The two first steady-state solutions for the solid phase are constant in each zone. Row 1 in Table 2 gives

$$\varphi_{\mathrm{SS1}}(z) := \begin{cases} \varphi_3 = 0 & \text{for } z_{\mathrm{W}} \le z < z_{\mathrm{E}}, \\ \varphi_2 = 0 & \text{for } z_{\mathrm{F}} \le z < z_{\mathrm{W}}, \\ \varphi_1 \in [0, \varphi_{1\mathrm{m}}] & \text{for } z_{\mathrm{U}} \le z < z_{\mathrm{F}}, \end{cases} \tag{5.2}$$

which requires (FIas) and (FJCs), and row 4 in Table 2 gives

$$\varphi_{\mathrm{SS2}}(z) := \begin{cases} \varphi_3 = 0 & \text{for } z_{\mathrm{W}} \le z < z_{\mathrm{E}}, \\ \varphi_2 = 0 & \text{for } z_{\mathrm{F}} \le z < z_{\mathrm{W}}, \\ \varphi_1 \in [\varphi_{1\mathrm{M}}, 1] & \text{for } z_{\mathrm{U}} \le z < z_{\mathrm{F}}, \end{cases} \tag{5.3}$$

which requires the additional conditions (CFIas), (FIbs) and (FJCs). The next solution has a discontinuity at $z = z_{\mathrm{d}}$ in zone 1 (couplings of row 1 in Table 2):

$$\varphi_{\mathrm{SS3}}(z) := \begin{cases} \varphi_3 = 0 & \text{for } z_{\mathrm{W}} \le z < z_{\mathrm{E}}, \\ \varphi_2 = 0 & \text{for } z_{\mathrm{F}} \le z < z_{\mathrm{W}}, \\ \varphi_1^{\uparrow} = \varphi_{1\mathrm{m}} & \text{for } z_{\mathrm{d}} \le z < z_{\mathrm{F}}, \\ \varphi_1^{\downarrow} = \varphi_{1\mathrm{M}} & \text{for } z_{\mathrm{U}} \le z < z_{\mathrm{d}}. \end{cases}$$

This solution requires the jump condition (FJCs) and is in fact the most wanted one in a clarifier-thickener, where the discontinuity at $z = z_{\mathrm{d}}$ is called sludge blanket level in wastewater treatment and sediment level in mineral processing.

There are other steady states possible, however, not desired, for example:

$$\varphi_{\mathrm{SS}}(z) := \begin{cases} \varphi_3 = 0 & \text{for } z_{\mathrm{W}} \le z < z_{\mathrm{E}}, \\ \varphi_2^{\uparrow} = 0 & \text{for } z_{\mathrm{d1}} \le z < z_{\mathrm{W}}, \\ \varphi_2^{\downarrow} = \varphi_{2\mathrm{Z}} & \text{for } z_{\mathrm{F}} \le z < z_{\mathrm{d1}}, \\ \varphi_1^{\uparrow} = \varphi_{1\mathrm{m}} & \text{for } z_{\mathrm{d2}} \le z < z_{\mathrm{F}}, \\ \varphi_1^{\downarrow} = \varphi_{1\mathrm{M}} & \text{for } z_{\mathrm{U}} \le z < z_{\mathrm{d2}}. \end{cases}$$

This requires conditions (FIVs) and (FJCs) according to the first coupling of row 2, which means that excessively large volumetric flows have to be used. In addition, there is no point (at least for the intended operation of a flotation column) in having a layer of particles standing still in the lower part of zone 2.

5.3. *Steady states of the solid phase in the case* ϕ_{SS2}

According to (CWW), ϕ_{SS2} requires (FIIIa) and $Q_{\mathrm{W}} = 0$; hence there is no spatial discontinuity at $z = z_{\mathrm{W}}$ between zones 2 and 3. The two first desired steady-state solutions for the solid phase are constant in each zone and the jump condition (FJCs) holds. Row 1 in Table 2 gives that φ_{SS1} is a solution under the additional condition (FIas). Row 2 in Table 2 gives that φ_{SS2} is a solution with the necessary conditions (CFIas), (FIbs), (WIs), (FIIs) and (FIIIs). A third possible solution is φ_{SS3}, which requires the jump condition (FJCs). A fourth steady-state solution, which has a discontinuity at $z = z_{\mathrm{d}}$ in zone 2, is

$$\varphi_{\mathrm{SS4}}(z) := \begin{cases} \varphi_3 = 0 & \text{for } z_{\mathrm{W}} \le z < z_{\mathrm{E}}, \\ \varphi_2^{\uparrow} = 0 & \text{for } z_{\mathrm{d}} \le z \le z_{\mathrm{W}}, \\ \varphi_2^{\downarrow} = \varphi_{2\mathrm{Z}} & \text{for } z_{\mathrm{F}} \le z < z_{\mathrm{d}}, \\ \varphi_1 = \varphi_2^{\downarrow} \in [\varphi_{1\mathrm{M}}, 1] & \text{for } z_{\mathrm{U}} \le z < z_{\mathrm{F}}, \end{cases}$$

which requires also (WIs), see row 5 in Table 2. The region in zone 2 with the volume fraction $\varphi_{2\mathrm{Z}}$ consists of solids at rest.

5.4. *Steady states of the solid phase in the case* ϕ_{SS3}

According to (WW), ϕ_{SS3} requires (CFIIIa) and $Q_{\mathrm{W}} > 0$. We consider the fluxes of the solid phase above and below the discontinuity in zone 2 at z_{d} and let

$$g_{\mathrm{L}}(\varphi) = f_2(\varphi, \phi_2^{\uparrow}) = (1 - \phi_2^{\uparrow}) f_{\mathrm{b}}(\varphi) + \big(j_2(\phi_2^{\uparrow}) - q_2\big)\varphi,$$
$$g_{\mathrm{R}}(\varphi) = f_2(\varphi, \phi_2^{\downarrow}) = (1 - \phi_2^{\downarrow}) f_{\mathrm{b}}(\varphi) + \big(j_2(\phi_2^{\downarrow}) - q_2\big)\varphi.$$

The stationary discontinuity in ϕ satisfies $j_2(\phi_2^{\uparrow}) = j_2(\phi_2^{\downarrow})$; hence, the graphs of g_{L} and g_{R} intersect precisely at $\varphi = 0$ and $\varphi = 1$. Since $\phi_2^{\downarrow} \le \phi_2^{\uparrow}$, $g_{\mathrm{L}} \le g_{\mathrm{R}}$. With $\varphi_2^{\uparrow}$ and $\varphi_2^{\downarrow}$ denoting the values above and below $z = z_{\mathrm{d}}$, and $\varphi_{2\mathrm{Z}}^{\downarrow}$ referring to the function $f_2(\cdot, \phi_2^{\downarrow})$, we have the following possibilities:

(a) $\varphi_2^{\uparrow} = \varphi_2^{\downarrow} = 0$. Possible steady-state solutions for the the solid phase are φ_{SSk}, $k = 1, 2, 3$.
(b) $\varphi_2^{\uparrow} = 0$ and $\varphi_2^{\downarrow} = \varphi_{2\mathrm{Z}}^{\downarrow}$. A possible candidate solution is φ_{SS4}; however, row 5 of Table 2 gives the condition (FIIIa), which contradicts (CFIIIa). Hence, there exists no steady-state solution in this case.
(c) $\varphi_2^{\uparrow} \in [\varphi_{2\mathrm{Z}}^{\uparrow}, 1]$ and $\varphi_2^{\downarrow} \in [\varphi_{2\mathrm{Z}}^{\downarrow}, 1]$. Such a jump could occur in a variant of φ_{SS4} with a possible discontinuity between $\varphi_2^{\uparrow}$ and $\varphi_2^{\downarrow}$ in $z_{\mathrm{F}} < z < z_{\mathrm{d}}$. However, row 5 of Table 2 gives condition (FIIIa) for $\varphi_{2\mathrm{Z}}^{\uparrow}$ and $\varphi_{2\mathrm{Z}}^{\downarrow}$ to exist. Since this contradicts (CFIIIa), there exists no steady-state solution in this case.

6. Operating charts for desired steady states

We assume that ϕ_{F} and$\phi_{\mathrm{s,F}}$ are given and will present restrictions on the control variables Q_{F}, Q_{U} and Q_{W} for each qualitatively possible desired steady state. Many inequalities can be visualized as two-dimensional regions in the $(Q_{\mathrm{U}}, Q_{\mathrm{F}})$-plane which we call operating charts. Other conditions involve the triple $(Q_{\mathrm{U}}, Q_{\mathrm{F}}, Q_{\mathrm{W}})$, and in some cases, also the solution value ϕ_2 in zone 2. The equality conditions for the desired steady states of the aggregate phase are the jump conditions (FJC) and (WJC), which reduce to the following:

$$Q_{\mathrm{F}}\phi_{\mathrm{F}} = A_{\mathrm{E}} j_2(\phi_2; Q_2/A_{\mathrm{E}}), \tag{FJC}$$

$$A_{\mathrm{E}} j_2(\phi_2; Q_2/A_{\mathrm{E}}) = A_{\mathrm{E}} j_3(\phi_3; (Q_2 + Q_{\mathrm{W}})/A_{\mathrm{E}}). \tag{WJC}$$

We need the following lemma for the construction of operating charts, in which the operator can choose a point $(Q_{\mathrm{U}}, Q_{\mathrm{F}})$. Then $Q_2 = -Q_{\mathrm{U}} + Q_{\mathrm{F}}$ is given.

Lemma 6.1. *The jump conditions* (FJC) *and* (WJC) *for the desired steady states imply the following for given* $(Q_{\mathrm{U}}, Q_{\mathrm{F}})$*:*

1. *Condition* (FJC) *gives at most one* ϕ_2 *in each of the intervals* $(0, \phi^{\mathrm{M}}(Q_2/A_{\mathrm{E}})]$, $[\phi^{\mathrm{M}}(Q_2/A_{\mathrm{E}}), \phi_{\mathrm{M}}(Q_2/A_{\mathrm{E}})]$ *and* $[\phi_{\mathrm{M}}(Q_2/A_{\mathrm{E}}), \phi_{\max}]$.
2. *In the case* (CWW)*,* ϕ_3 *is determined as in 1.*
3. *In the case* (WW)*,* $\phi_3 = \phi_{3\mathrm{M}} = \phi_{\mathrm{M}}((Q_2 + Q_{\mathrm{W}})/A_{\mathrm{E}})$ *and* (WI) *and* (E) *are satisfied. Furthermore,* Q_{W} *is uniquely determined as the solution of*

$$U := A_{\mathrm{E}} j_3\left(\phi_{\mathrm{M}}\left(\frac{-Q_{\mathrm{U}} + Q_{\mathrm{F}} + Q_{\mathrm{W}}}{A_{\mathrm{E}}}\right); \frac{-Q_{\mathrm{U}} + Q_{\mathrm{F}} + Q_{\mathrm{W}}}{A_{\mathrm{E}}}\right) - Q_{\mathrm{F}}\phi_{\mathrm{F}} = 0. \tag{6.1}$$

Proof. Statement 1 follows directly from the concave-convex property of the flux function j_2. Then the second statement follows directly. In the third statement, (WI) is satisfied since (WJC) implies

$$j_2(\phi_2^{\mathrm{M}}) \geq j_2(\phi_2) = j_3(\phi_{3\mathrm{M}}).$$

The boundary of condition (E) is the straight line $-Q_{\mathrm{U}} + Q_{\mathrm{W}} + Q_{\mathrm{F}} = 0$, which for fixed Q_{W} is a contour in the $(Q_{\mathrm{U}}, Q_{\mathrm{F}})$-plane with gradient $(-1, 1)$. The line passes

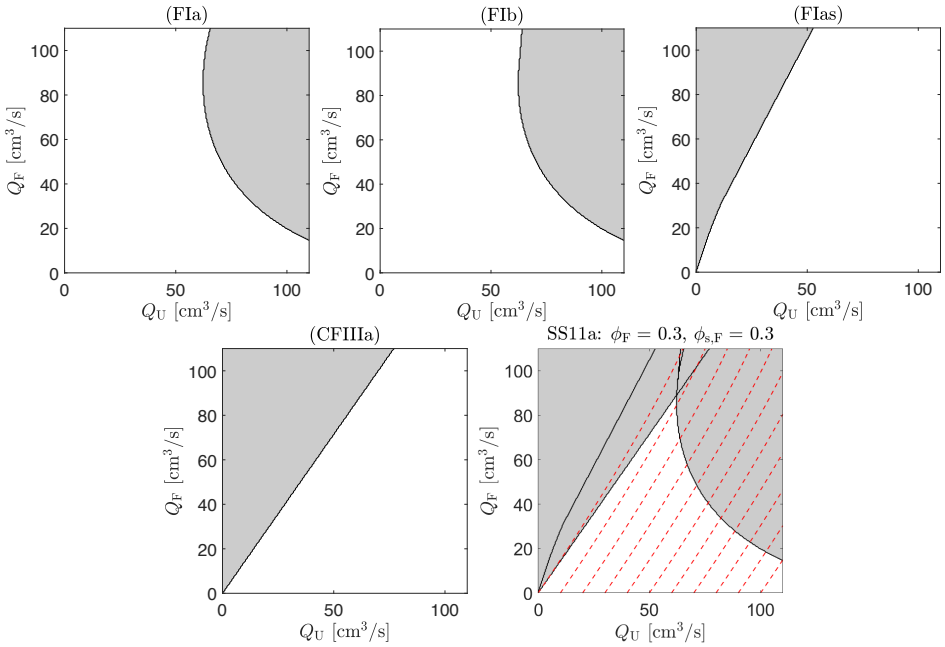

Fig. 8. Operating charts in the case SS11a with $\phi_F = 0.3$ and $\phi_{s,F} = 0.3$. The four first plots show where each condition is satisfied (white regions). The last plot shows all four conditions superimposed and curves (red dashed) a long which Q_W is constant with $Q_W = 0, 10, 20, \ldots$ cm^3/s. The value of Q_W can be read off on the Q_U-axis.

the point $(Q_W, 0)$ and so does the curve defined implicitly by (6.1). The points on the curve satisfy (E) since the gradient of U is

$$\left(\frac{\partial U}{\partial Q_U}, \frac{\partial U}{\partial Q_F}\right) = A_E\left(-\phi_{3M}, \phi_{3M} - \phi_F\right)\frac{1}{A_E} = \phi_{3M}\left(-1, 1 - \frac{\phi_F}{\phi_{3M}}\right),$$

where we use Lemma 2.1. That Q_W is uniquely determined by (6.1) for given (Q_U, Q_F) follows from the implicit function theorem, since

$$\frac{\partial U}{\partial Q_W} = A_E\phi_{3M}\frac{1}{A_E} = \phi_M(Q_E/A_E),$$

which is strictly positive when $Q_E > 0$, i.e., when (E) holds. □

For the desired steady states of the solid phase, condition (WJCs) is satisfied with $\varphi_3 = 0$ and either $\varphi_2 = 0$ or $\varphi_2 = \varphi_{2Z}$, and the one at the feed inlet is

$$A_U f_1(\varphi_1, 0; -Q_U/A_U) = Q_F\phi_{s,F}. \qquad \text{(FJCs)}$$

6.1. *Case SS11: ϕ_{SS1} and φ_{SS1}*

According to (WW), wash water is present and from (3.9), (5.2), row 2 in Table 1 and row 1 in Table 2, we get the following:

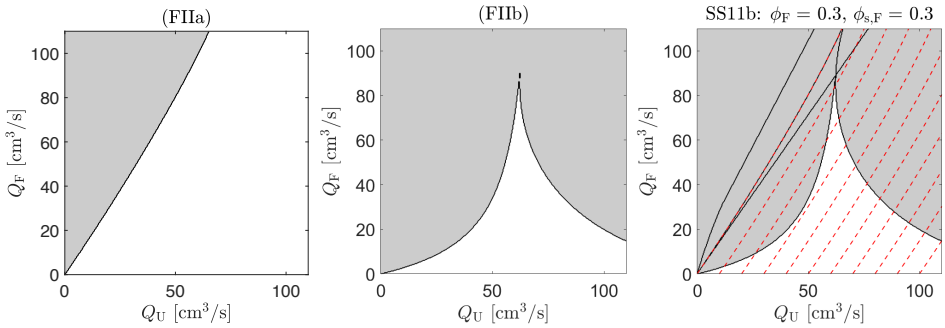

Fig. 9. Operating charts in the case SS11b with $\phi_F = 0.3$ and $\phi_{s,F} = 0.3$. The conditions (FIIa) and (FIIb) are shown (see Figure (8) for others), and in the third plot all conditions together with the red dashed lines showing the values of $Q_W = 0, 10, 20, \ldots$ cm^3/s.

(a) The case $\phi_2 \in [\phi_{2m}, \phi_2^M]$: The conditions are set of inequalities (FIa), (FIb), (FIas), (CFIIIa), (WI) and (E) along with the jump conditions. The first four conditions involve only Q_U and Q_F, and these conditions are visualized in Fig. 8 for the choice $\phi_F = 0.3$ and $\phi_{s,F} = 0.3$. The white region in the fifth subplot of Fig. 8 shows the possible values for (Q_U, Q_F). For each such point, Lemma 6.1 gives that Q_W is uniquely determined. In the fifth subplot of Fig. 8, we have, for fixed values of $Q_W = 0, 10, 20, \ldots$ cm^3/s, drawn the corresponding curves (dashed red) defined by (6.1). The value of Q_W for a curve can be read off at the curve's intersection with the Q_U-axis. This is because $Q_F = 0$ in (6.1) gives $\phi_M(-Q_U + Q_W) = \phi_{max}$, which is equivalent to $Q_W = Q_U$. For any chosen point (Q_U, Q_F) in the white region of the fifth subplot of Fig. 8, Lemma 6.1 gives that (WI) and (E) are satisfied. One can for example choose the point $(Q_U, Q_F) = (55, 70)$ cm^3/s and solve (6.1) for $Q_W \approx 10.86$ cm^3/s.

(b) The case $\phi_2 \in [\phi_2^M, \phi_{2M}]$: The conditions are (FIa), (FIIa), (FIIb), (FIas), (CFIIIa), (WI), (E) and the jump conditions. For $\phi_F = 0.3$ and $\phi_{s,F} = 0.3$ we get the regions shown in Fig. 9, where we show the new conditions in comparison with subcase (a).

6.2. *Case SS12:* ϕ_{SS1} *and* φ_{SS2}

According to (WW), wash water is present and from (3.9), (5.3), row 2 in Table 1 and row 4 in Table 2, we get the following:

(a) The case $\phi_2 \in [\phi_{2m}, \phi_2^M]$: The set of conditions are (FIa), (FIb), (CFIas), (FIbs), (CFIIIa), (WI), (E) and (WJC). The first five conditions involve only Q_U and Q_F, and these conditions are visualized in Fig. 10 for the choice $\phi_F = 0.2$ and $\phi_{s,F} = 0.6$. For low values of $\phi_{s,F}$ this steady state does not exist. The wedge-shaped white region in the sixth subplot of Fig. 10 shows the necessary region

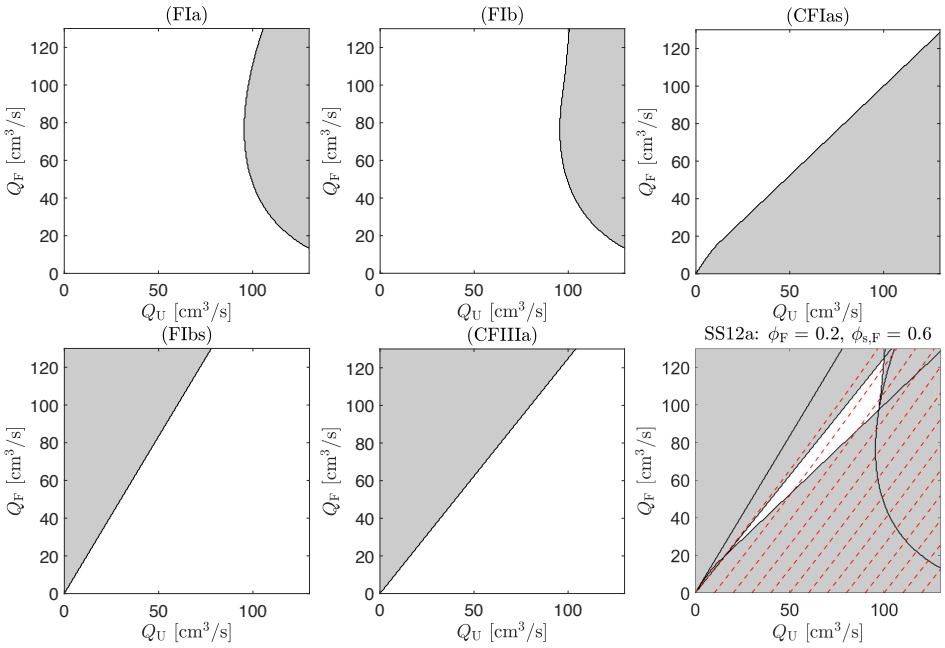

Fig. 10. Operating charts in the case SS12a with $\phi_F = 0.2$ and $\phi_{s,F} = 0.6$ and $\phi_2 \in [\phi_{2m}, \phi_2^M]$. The five first plots show where each condition is satisfied (white region). The sixth plot shows all conditions superimposed and the dashed red lines show the corresponding values of $Q_W = 0, 10, 20, \ldots$ cm^3/s.

for (Q_U, Q_F). Lemma 6.1 gives that (WI) and (E) are satisfied, and the curves for $Q_W = 0, 10, 20, \ldots$ cm^3/s given by (6.1) have been drawn. Condition (CFIas) is the region above the curve $Q_F = X(Q_U)$ which has the derivative (we use Lemma 2.1)

$$X'(Q_U) = \frac{\varphi_M(Q_U/A_U)}{\phi_{s,F}}.$$

The numerator decreases with Q_U from $\varphi_M(0) = 1$ to $\varphi_M(\varphi_{infl}) = 0.5714$. This explains why a non-empty (white) region exists only for large values of $\phi_{s,F}$. The convex Q_W-curves give that we can choose, for example, $(Q_U, Q_F) = (40, 45)$ cm^3/s and then (6.1) gives $Q_W = 5.1716$ cm^3/s.

(b) The case $\phi_2 \in [\phi_2^M, \phi_{2M}]$: The conditions are (FIa), (FIIa), (FIIb), (CFIas), (FIbs), (CFIIIa), (WI), (E) and (WJC). We can only find this steady state when there is only a small amount of fluid in the feed inlet. With $\phi_F = 0.4$ and $\phi_{s,F} = 0.5$, Fig. 11 shows condition (FIIa) and all conditions combined.

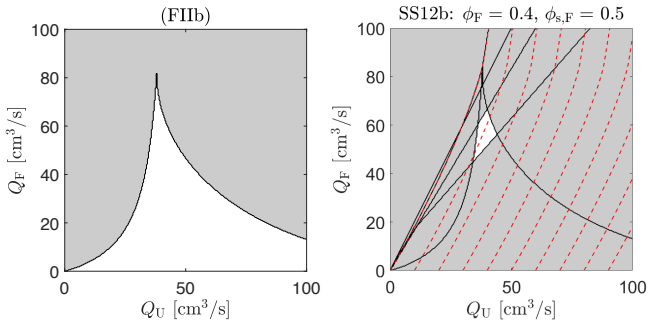

Fig. 11. Operating charts in the case SS12b with $\phi_F = 0.4$ and $\phi_{s,F} = 0.5$ and $\phi_2 \in [\phi_2^M, \phi_{2M}]$.

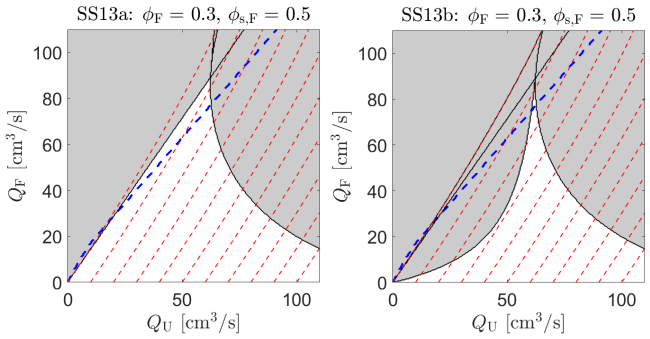

Fig. 12. Operating charts in the cases SS13a and SS13b.

6.3. *Case SS13: ϕ_{SS1} and φ_{SS3}*

According to (WW), wash water is used, ϕ_{SS1} is given by (3.9) (see row 2 in Table 1) and φ_{SS3} by (5.3) (row 1 in Table 2), where the jump condition (FJCs) is condition (FIas) with equality:

$$A_U f\big(\varphi_{1M}(Q_U/A_U), 0, -Q_U/A_U\big) = Q_F \phi_{s,F}. \tag{FIase}$$

For given $\phi_{s,F}$, this is a curve in the (Q_U, Q_F)-plane shown in dashed blue in Fig. 12. As in the previous subcases, Lemma 6.1 and imply that (WI), (E) and (WJC) are satisfied along the shown red dashed lines. We have the following two subcases:

(a) The case $\phi_2 \in [\phi_{2m}, \phi_2^M]$: The inequality conditions are (FIa), (FIb) and (CFIIIa); see Fig. 12 (left), which is drawn in the case $\phi_F = 0.3$ and $\phi_{s,F} = 0.5$. In order to obtain a discontinuity of solid particles in zone 1, there has to be a large feed volume fraction of solids for this steady state to exist.

(b) The inequality conditions are $\phi_2 \in [\phi_2^M, \phi_{2M}]$: The conditions are (FIa), (FIIa), (FIIb) and (CFIIIa). A solution exists only when the feed inlet contains a very small amount of fluid, see Figure 12 (right) for $\phi_F = 0.4$ and $\phi_{s,F} = 0.5$.

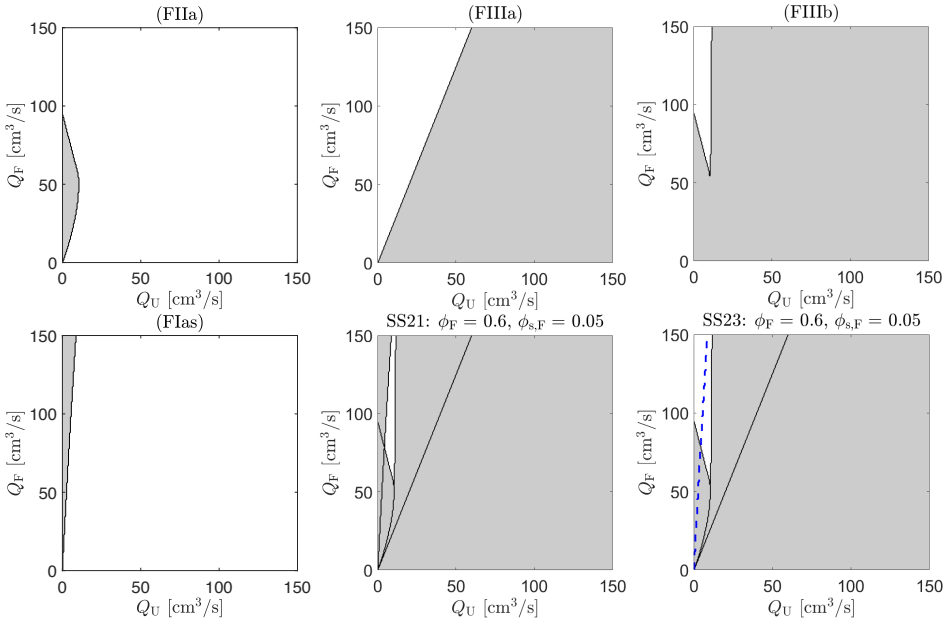

Fig. 13. Operating charts in the cases SS21 and SS23. In the last plot, the possible values for (Q_U, Q_F) are on the blue dashed line in the white region.

6.4. *Case SS21:* ϕ_{SS2} *and* φ_{SS1}

According to (CWW), $Q_W = 0$, and ϕ_{SS2} requires (FIIa), (FIIIa), (FIIIb) and (WII). Since $j_2 \equiv j_3$, (WII) is equivalent to $Q_2 \geq 0$, and in this case (E), which is implied by (FIIIa). Row 1 in Table 2 gives that φ_{SS1} requires (FIas). Lemma 6.1 states that the jump conditions determine $\phi_2 = \phi_3 \in [\phi_{2M}, 1]$ uniquely without any further restriction on the volumetric flows. Analogously, $\varphi_1 \in [\varphi_{1M}, 1]$ is determined by (FJCs) without any restriction on the volumetric flows. The inequality conditions (FIIa), (FIIIa), (FIIIb) and (FIas) are shown in Fig. 13 for $\phi_F = 0.6$ and $\phi_{s,F} = 0.05$. This steady state exists only for small $\phi_{s,F}$, but can handle large Q_F.

6.5. *Case SS22:* ϕ_{SS2} *and* φ_{SS2}

According to (CWW), $Q_W = 0$, and ϕ_{SS2} requires (FIIa), (FIIIa), (FIIIb) and (WII). As in the previous case, (FIIIa) implies (WII) and (E), and the jump conditions give no specific constraint on the volumetric flows. Row 3 in Table 2 gives that φ_{SS2} requires the inequality conditions (CFIas), (FIbs), (WIs), (FIIs) and (FIIIs). There are thus eight inequality conditions and we cannot find any non-empty region for any choices of ϕ_F and $\phi_{s,F}$.

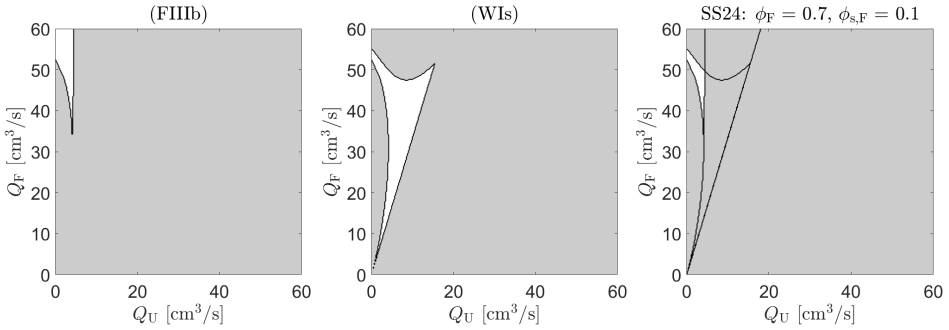

Fig. 14. Operating charts in the case SS24.

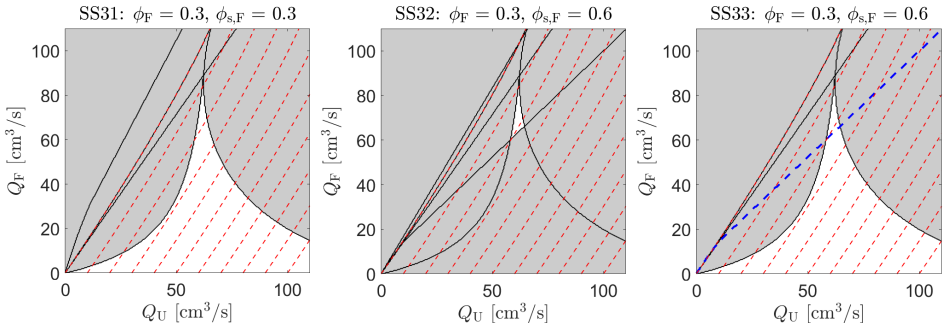

Fig. 15. Operating charts in the cases SS31, SS32 and SS33.

6.6. *Case SS23:* ϕ_{SS2} *and* φ_{SS3}

As in the previous two cases, (CWW) gives $Q_W = 0$. The solution ϕ_{SS2} requires (FIIa), (FIIIa) (which implies (WII) and (E)) and (FIIIb), and φ_{SS3} requires the equality condition (FIase). The latter condition sharpens case SS21, see the last plot of Fig. 13.

6.7. *Case SS24:* ϕ_{SS2} *and* φ_{SS4}

As in the previous two cases, (CWW) gives $Q_W = 0$. The solution ϕ_{SS2} requires (FIIa), (FIIIa) (which implies (WII) and (E)) and (FIIIb), while φ_{SS4} requires only (WIs). A non-empty regions is found only for large ϕ_F, see Fig. 14.

6.8. *Case SS31:* ϕ_{SS3} *and* φ_{SS1}

Condition (WW) gives that wash water can be used and (CFIIIa) holds. The solution ϕ_{SS3} requires the inequality conditions (FIa), (FIIa), (FIIb) and (WI), and row 1 in Table 2 give that φ_{SS1} requires the additional condition (FIas). Lemma 6.1 gives

partly that (WI) and (E) are satisfied, and partly that the jump conditions give the value of Q_{W} from (6.1). Fig. 15 (left) shows the operating charts for $\phi_{\mathrm{F}} = 0.3$ and $\phi_{\mathrm{s,F}} = 0.3$.

6.9. *Case SS32: ϕ_{SS3} and φ_{SS2}*

Condition (WW) gives that wash water can be used and (CFIIIa) holds. The solution ϕ_{SS3} requires the inequalities (FIa), (FIIa), (FIIb) and (WI), and φ_{SS2} requires the additional conditions (CFIas) and (FIbs). Lemma 6.1 gives partly that (WI) and (E) are satisfied, and partly that the jump conditions give the value of Q_{W} from (6.1). A non-empty region can be found only when there is hardly any fluid and lots of solids in the feed inlet; see Fig. 15 (middle) when $\phi_{\mathrm{F}} = 0.3$ and $\phi_{\mathrm{s,F}} = 0.6$. Hence, this solution is not of practical interest.

6.10. *Case SS33: ϕ_{SS3} and φ_{SS3}*

Condition (WW) gives that wash water can be used and (CFIIIa) holds. The solution ϕ_{SS3} requires the inequalities (FIa), (FIIa), (FIIb) and (WI), and φ_{SS3} requires the equality condition (FIase). The latter equality means an additional restriction to the conditions of case SS31; see Fig. 15 (right), where the blue dashed line for condition (FIase) crosses the white region only for high values of $\phi_{\mathrm{s,F}}$.

7. Numerical simulations

7.1. *Numerical method*

For the discretization of the model, we exploit that our system of balance laws (1.1) is triangular. In Ref. 9, the numerical scheme is described and an invariant region property proved. The scheme uses a staggered grid for the two unknown functions ϕ and φ of (1.1). The Godunov method is used first to obtain a piecewise constant, in space and time, approximation $\phi^{\Delta z}$ of the solution ϕ of the first PDE of (1.1). Then $\phi^{\Delta z}$ is used as a given function in the second PDE of (1.1). By using a staggered grid for the numerical approximation of φ, the spatially dependent $\phi^{\Delta z}$ is constant in a neighbourhood of the cell boundaries and the Godunov flux is well defined. For the same reason, the two grids should preferably be placed so that the known spatial discontinuities at z_{U}, z_{F}, z_{W} and z_{E} lie inside cells of both grids.

More precisely, we let N cells for each grid cover the column, so that cell no. 1 contains z_{U} and cell no. N contains z_{E}; see Figure 16. We add extra cells at the bottom and top to calculate the outlet volume fractions. We define $\Delta z := 1/N$, $z_i := i\Delta z$, $i = -1, -1/2, 0, 1/2, \ldots, N+2$, so that $z_{\mathrm{U}} = z_1 + \Delta z/4$ and $z_{\mathrm{E}} = z_N + \Delta z/4$. Each of the injection points z_{F} and z_{W} will belong to one interval of each grid. The numerical method implicitly assumes that these two locations are placed a distance $\Delta z/4$ from the nearest boundary of both grids. The time discretization is made with the uniform step length Δt, which should satisfy a Courant-Friedrichs-Lewy (CFL)

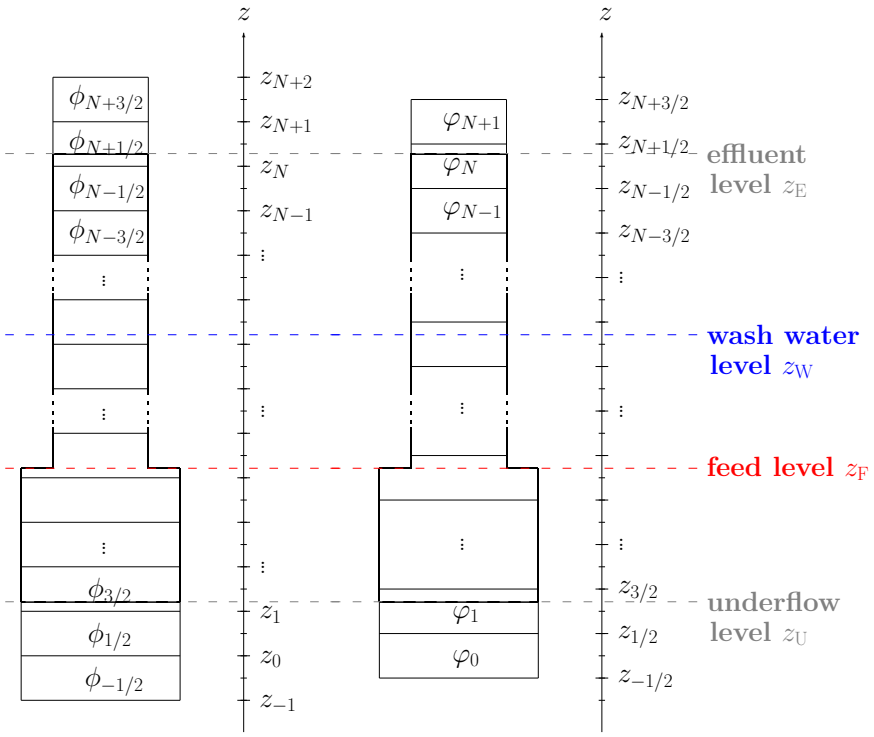

Fig. 16. Two staggered grids for the discretization of the flotation column with the spatial discontinuities away from cell boundaries.

condition; see below. We simulate N_T time steps up to the final time $T := N_T \Delta t$ and $t^n := n\Delta t$ for $n = 0, 1, \ldots, N_T$.

We allow $A(z)$ to have a finite number of discontinuities and this function is discretized as follows:

$$A_{i+1/2} := \frac{1}{\Delta z} \int_{z_i}^{z_{i+1}} A(z)\,\mathrm{d}z, \qquad A_i := \frac{1}{\Delta z} \int_{z_{i-1/2}}^{z_{i+1/2}} A(z)\,\mathrm{d}z.$$

The CFL condition is the following:

$$\begin{aligned} &\Delta t\, M \left(\|f_{\mathrm{b}}'\|_\infty + \|j_{\mathrm{b}}'\|_\infty + \frac{\|Q\|_\infty}{A_{\min}} \right) \le \frac{\Delta z}{2}, \quad \text{where} \\ &M := \max_{i=0,1/2,1,\ldots,N+1} \left\{ \frac{A_{i-1/2}}{A_i}, \frac{A_{i+1/2}}{A_i} \right\}, \quad \|f_{\mathrm{b}}'\|_\infty := \max_{0\le\phi\le 1} |f_{\mathrm{b}}'(\phi)|, \\ &\|Q\|_\infty := \max_{0\le t\le T} (Q_{\mathrm{F}}(t) + Q_{\mathrm{W}}(t)), \quad A_{\min} := \min_{i=-1/2,0,1/2,\ldots,N+3/2} A_i. \end{aligned} \tag{7.1}$$

The time-dependent feed functions are discretized as

$$Q_{\mathrm{F}}^n := \frac{1}{\Delta t} \int_{t^n}^{t^{n+1}} Q_{\mathrm{F}}(t)\,\mathrm{d}t, \qquad \phi_{\mathrm{F}}^n := \frac{1}{\Delta t} \int_{t^n}^{t^{n+1}} \phi_{\mathrm{F}}(t)\,\mathrm{d}t,$$

and the same is made for the other volumetric flows and $\phi_{\mathrm{s,F}}$. We define the dimensionless function

$$\delta_{\mathrm{F},i+1/2} := \int_{z_i}^{z_{i+1}} \delta_{z_{\mathrm{F}}}(z)\,\mathrm{d}z := \begin{cases} 1 & \text{if } z_{\mathrm{F}} \in [z_i, z_{i+1}), \\ 0 & \text{otherwise.} \end{cases}$$

We use the flux by Godunov,[31] which, for a given flux function g and real values a and b on the left/right, is

$$G(g,a,b) = \begin{cases} \min\limits_{a\le\phi\le b} g(\phi) & \text{if } a \le b, \\ \max\limits_{a\ge\phi\ge b} g(\phi) & \text{if } a > b. \end{cases} \tag{7.2}$$

The numerical approximations of the PDE solutions are denoted by $\phi^n_{i+1/2} \approx \phi(z_{i+1/2}, t^n)$ and $\varphi^n_i \approx \varphi(z_i, t^n)$. More precisely, the initial data are discretized by

$$\phi^0_{i+1/2} := \frac{1}{A_{i+1/2}\Delta z}\int_{z_i}^{z_{i+1}} \phi(z,0)A(z)\,\mathrm{d}z, \quad \varphi^0_i := \frac{1}{A_i\Delta z}\int_{z_{i-1/2}}^{z_{i+1/2}} \varphi(z,0)A(z)\,\mathrm{d}z,$$

and the scheme (marching formula) is

$$\phi^{n+1}_{i+1/2} = \phi^n_{i+1/2} + \frac{\Delta t}{A_{i+1/2}\Delta z}\left(A_i\mathcal{J}^n_i - A_{i+1}\mathcal{J}^n_{i+1} + Q^n_{\mathrm{F}}\phi^n_{\mathrm{F}}\delta_{\mathrm{F},i+1/2}\right), \tag{7.3}$$

$$\varphi^{n+1}_i = \begin{cases} \varphi^n_i & \text{if } \bar\phi^n_i = 1, \\ \varphi^n_i + \dfrac{\Delta t(A_{i-1/2}\mathcal{F}^n_{i-1/2} - A_{i+1/2}\mathcal{F}^n_{i+1/2} + Q^n_{\mathrm{F}}\phi^n_{\mathrm{s,F}}\delta_{\mathrm{F},i})}{(1-\bar\phi^n_i)\Delta z\, A_i} & \text{otherwise,} \end{cases} \tag{7.4}$$

where $\bar\phi^n_i := (\phi^n_{i-1/2} + \phi^n_{i+1/2})/2$ and

$$\mathcal{J}^n_i := G\big(J(\cdot, z_i, t^n), \phi^n_{i-1/2}, \phi^n_{i+1/2}\big),$$
$$\mathcal{F}^n_{i+1/2} := -G\big(F(\cdot, \phi^n_{i+1/2}, z_{i+1/2}, t^n), \varphi^n_{i+1}, \varphi^n_i\big).$$

In the numerical flux $\mathcal{J}^n_i$, we replace $A(z_i)$ by A_i, and analogously for $\mathcal{F}^n_{i+1/2}$.

We define an approximate solution for the solids volume fraction ϕ_{s} by

$$\phi^{n+1}_{\mathrm{s},i} := \left(1 - \overline{\phi^n_i}\right)\varphi^{n+1}_i \quad \text{for all } i, n,$$

and the piecewise constant approximate solution on $\mathbb{R}\times[0,T)$ as follows, where χ_Ω is the characteristic function of the set Ω:

$$\phi^{\Delta z}(z,t) := \sum_{i,n} \chi_{[z_i, z_{i+1})}(z)\chi_{[t^n, t^{n+1})}(t)\phi^n_{i+1/2},$$
$$\phi^{\Delta z}_{\mathrm{s}}(z,t) := \sum_{i,n} \chi_{[z_{i-1/2}, z_{i+1/2})}(z)\chi_{[t^n, t^{n+1})}(t)\phi^n_{\mathrm{s},i}.$$

In work under preparation we prove properties of the scheme defined by the update formulas (7.3) and (7.4), and apply variants of it to other models. Roughly speaking, the main result can be formulated by the following theorem. Its proof

is presented in Ref. 9. The key property that needs to be established to prove the statement is the monotonicity of the update formulas (7.3) and (7.4).

Theorem 7.1. *Assume that* $\Delta t > 0$ *and* $\Delta z > 0$ *are chosen such that the CFL condition* (7.1) *is in effect. If the initial data satisfy* $0 \le \phi(z,0), \phi_{\mathrm{s}}(z,0) \le 1$*, then the scheme* (7.3), (7.4) *produces approximate solutions that satisfy the invariant region property*

$$0 \le \phi^{\Delta z}(z,t), \phi_{\mathrm{s}}^{\Delta z}(z,t) \le 1 \quad \text{for } (z,t) \in \mathbb{R} \times [0,T). \tag{7.5}$$

7.2. *Numerical examples*

We use the functions j_{b} and f_{b} given by (2.13) and (2.14), respectively, with the parameters and functions V_{asus} and V_{sf} specified in Section 2.5. The height of the vessel is 100 cm measured from $z_{\mathrm{U}} = 0$ cm and we have placed the injection points at $z_{\mathrm{F}} = 33.3$ cm and $z_{\mathrm{W}} = 66.7$ cm, dividing the tank into three zones with the same height.

7.2.1. *Example 1.*

In this first example we consider a column filled only with fluid at time $t = 0$ s, hence $\phi(z,0) = \phi_{\mathrm{s}}(z,0) = 0$ for all z, when we start feeding aggregates, solids, fluid and wash water at their corresponding inlets, with $\phi_{\mathrm{F}} = 0.3$ and $\phi_{\mathrm{s,F}} = 0.3$. We choose the volumetric flows so that $(Q_{\mathrm{U}}, Q_{\mathrm{F}}) = (62, 70)\,\mathrm{cm}^3/\mathrm{s}$ lies in the white region in the operating chart in Figure 8, so that a steady-state of type SS11a is feasible. Then $Q_{\mathrm{W}} = 17.86\,\mathrm{cm}^3/\mathrm{s}$ is calculated by (6.1) so that (WJC) is satisfied. These values imply that we have

$$q(z,t) = \begin{cases} q_1 = -0.741\,\mathrm{cm/s} & \text{for } z < z_{\mathrm{F}}, \\ q_2 = 0.111\,\mathrm{cm/s} & \text{for } z_{\mathrm{F}} \le z < z_{\mathrm{W}}, \\ q_3 = 0.358\,\mathrm{cm/s} & \text{for } z \ge z_{\mathrm{W}}, \end{cases} \qquad 0 \le t < 180, \quad t > 420\,\mathrm{s}.$$

Fig. 17 shows the time evolution of the volume fractions of the aggregate and solid phases, and Fig. 18 shows snapshots at four time points. Initially, the aggregates rise fast to the top while solids settle and a first steady state is almost reached after $t = 180$ s, see Fig. 18(a). That steady state corresponds to row 1 of Table 1 and is not among the desired ones, since a froth layer at the top of the vessel is not obtained ($\phi_3 = \phi_{3\mathrm{m}} = 0.1465 < \phi_{3\mathrm{M}} = 0.7065$), which is not adequate for efficient desliming.

At $t = 180$ s, we close the top of the vessel by setting temporarily $Q_{\mathrm{U}} = Q_{\mathrm{F}} + Q_{\mathrm{W}}$ so that $Q_{\mathrm{E}} = 0\,\mathrm{cm}^3/\mathrm{s}$, and let the column be filled of aggregates until $t = 420$ s, when we open again the top of the column by setting the volumetric flows to their initial values. In Fig. 18(b) it can be seen that aggregates have travelled down, interacting with the solid phase in zone 1 and leaving the tank through the underflow outlet.

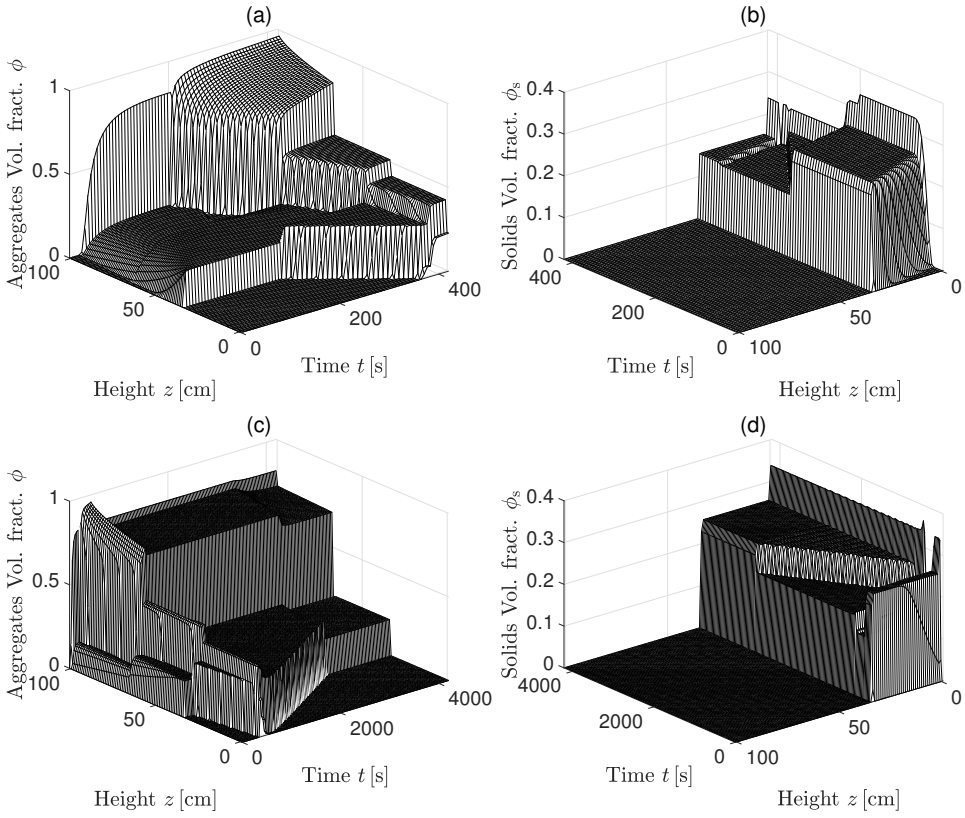

Fig. 17. Example 1: Time evolution of the volume fraction profiles of aggregates ϕ ((a) and (c)) and solids ϕ_s ((b) and (d)) during the first 420 s in the upper row and the entire simulation to $t = 4200$ s in the bottom row. Note the discontinuities in the volume fractions at the outlets.

After the top of the column is opened, there is an upwards moving discontinuity of aggregates in zone 1, below the feed inlet at $z = z_F = 33.3$ cm; see Fig. 18(c). Finally, as can be seen in Fig. 18(d), a second steady state is reached slowly after $t = 4200$ s, corresponding to a steady state of type SS11a, as it was expected.

7.2.2. *Example 2.*

From Figure 15 (left), we know that the volumetric flows chosen in Example 1, $(Q_U, Q_F) = (62, 70)\,\text{cm}^3/\text{s}$, also lie in the white region of the operating chart for steady states of type SS31. If at time $t = 4200$ s we close the tank just for 10 seconds, open it again at $t = 4210$ s and let the system evolve with time, following the same procedure as in the previous example, then we can see how a steady state of type SS31, with a stationary discontinuity of the aggregates volume fraction in zone 2, at

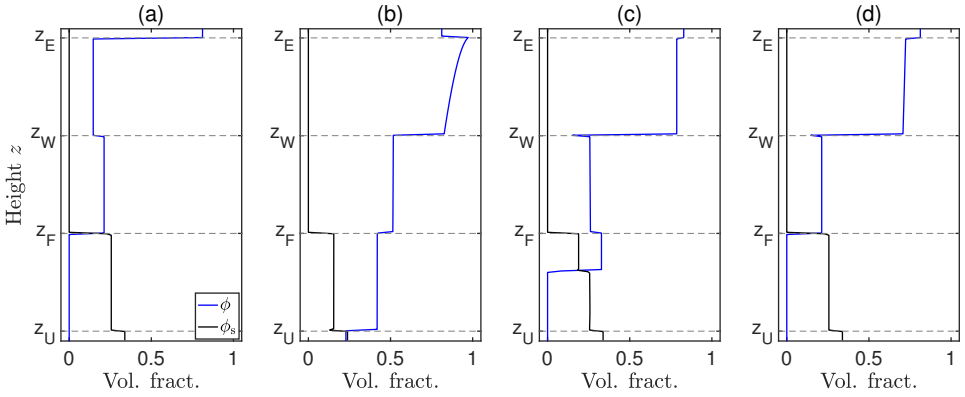

Fig. 18. Example 1: Volume fraction profiles of the aggregate ϕ and solid ϕ_s phases at (a) $t = 180\,\mathrm{s}$, (b) $t = 420\,\mathrm{s}$, (c) $t = 2000\,\mathrm{s}$ and (d) $t = 4200\,\mathrm{s}$.

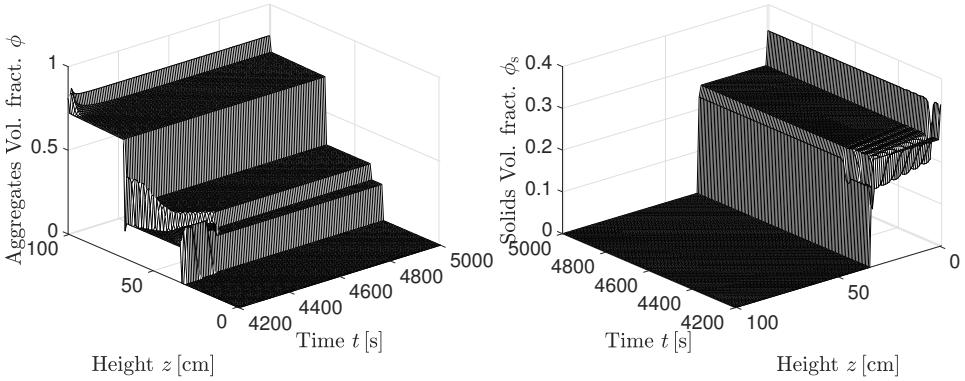

Fig. 19. Example 2: Time evolution of the volume fraction profiles of aggregates ϕ and solids ϕ_s starting from the end profile at $t = 4200\,\mathrm{s}$ of Example 1.

the point $z_d \in [z_F,\, z_W] = [33.3,\, 66.7]\,\mathrm{cm}$, is reached; see Figs. 19 and 20(d), with:

$$\begin{cases} \phi_2^{\uparrow} = 0.3057 \in [\phi_2^{M}, \phi_{2M}] = [0.2569, 0.8472] & \text{for } z_d \le z < z_W, \\ \phi_2^{\downarrow} = 0.2125 \in [\phi_{2m}, \phi_2^{M}] = [0.0401, 0.2569] & \text{for } z_F \le z < z_d, \end{cases}$$

satisfying $j_2(\phi_2^{\uparrow}) = j_2(\phi_2^{\downarrow})$.

8. Conclusions

A one-dimensional model is proposed for the hydrodynamic movement of simultaneously rising aggregates (air bubbles with attached hydrophobic particles) and settling hydrophilic particles in the fluid under in- and outflows of a flotation column. The model is a non-strictly hyperbolic, triangular system of two PDEs, whose

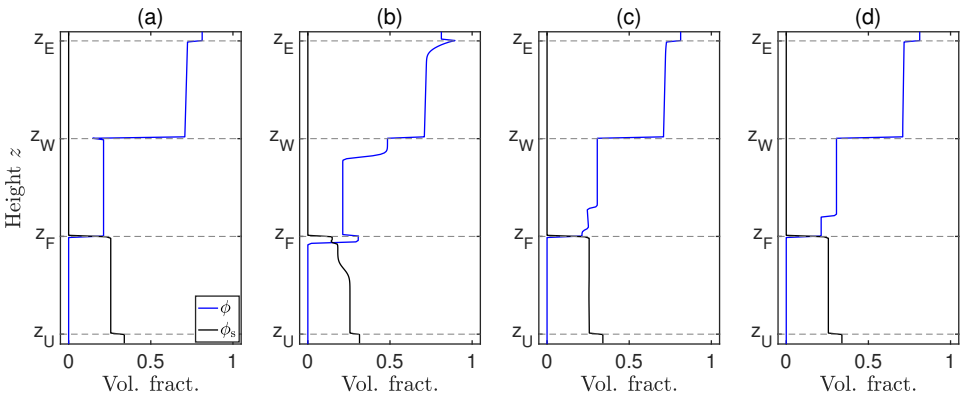

Fig. 20. Example 2: Volume fraction profiles of the aggregate ϕ and solid ϕ_s phases at (a) $t = 4200\,s$, (b) $t = 4210\,s$, (c) $t = 4350\,s$ and (d) $t = 5000\,s$.

flux functions have several spatial discontinuities due to the in- and outflows. The PDEs can in principle be solved consecutively. Each spatial discontinuity means that locally a scalar conservation law with discontinuous flux should be solved, first for the aggregate volume fraction, then with this solution as known coefficients in the second equation for the volume fraction of solids within the suspension.

The main results of this work are the derivation of the model equations and the categorization of steady-state solutions for a device called the Reflux Flotation Cell,[16,28] where the slurry of water and particles is mixed with air before the three phases are injected into the column. The classification of steady states; see Sections 3.4 and 5.2–5.4, is generic in the sense that it does not depend on the particular choices of the constitutive functions j_b and f_b. A numerical scheme is also suggested, which is able to handle more flexible geometries than in the examples presented here. The varying cross-sectional area $A(z)$ may be piecewise continuous.

The advantage of modelling three-phase flow with PDEs arising from fundamental basic principles is that established theory for PDEs can be used to obtain a complete description of all possible steady states. Although there are many theoretically possible steady states of our model, some of these are undesired due to large volumetric flows or layers of particles or aggregates standing still relative to the column. By imposing natural physical requirements, we obtain a reduction of all possible steady states to a few desired ones. In particular, the additional natural requirement that the use of wash water should be effective – it should flow downwards through the froth region below the wash water inlet – turns up as a one of the conditions in the categorization of steady states, namely (CFIIIa) in Section 4. In Section 5, we argue how this and other conditions lead to a natural division of the desired steady states of the aggregate phase into the two cases (WW), wash water is in effect, and (CWW), wash water is not injected since it would be flushed out at the top effluent.

The necessary nonlinear constraints on the volumetric flows for each steady state are visualized in operating charts for easy use of an operator. Among others, the capacity of the column is obtained in terms of an upper bound on the feed volumetric flow Q_{F} for given feed volume fractions ϕ_{F} and $\phi_{\mathrm{s,F}}$. Many steady states can only occur for large values on the sum $\phi_{\mathrm{F}} + \phi_{\mathrm{s,F}}$, which means that there is not much liquid in the feed inlet. Such are probably unrealistic steady states. For the most common steady states with froth in zones 2 and 3, and solid particles in zone 1, the operating charts give precise information on the limitations of the volumetric flows Q_{F}, Q_{U} and Q_{W} for given feed volume fractions ϕ_{F} and $\phi_{\mathrm{s,F}}$. Whether a steady state can be achieved or not depends also on the dynamic history, which we demonstrate with numerical simulations.

Our assumption that all aggregation of hydrophobic particles to bubbles occurs before the mixture of the three phases is fed into the column should be released in future work to allow for the aggregation process to occur also inside the column.

Acknowledgements

R.B. is supported by Fondecyt project 1170473; CRHIAM, Proyecto Conicyt/Fondap/15130015; CONICYT/PIA/Concurso Apoyo a Centros Científicos y Tecnológicos de Excelencia con Financiamiento Basal AFB170001; and by the INRIA Associated Team "Efficient numerical schemes for non-local transport phenomena" (NOLOCO; 2018–2020). M.C.M. is supported by Spanish MINECO grant MTM2017-83942-P.

References

1. B. Andreianov, K. H. Karlsen and N. H. Risebro, A theory of L^1-dissipative solvers for scalar conservation laws with discontinuous flux, *Arch. Ration. Mech. Anal.* (2011) 1–60.
2. D. Armbruster, S. Göttlich and M. Herty, A scalar conservation law with discontinuous flux for supply chains with finite buffers, *SIAM J. Appl. Math.* **71** (2011) 1070–1087.
3. O. A. Bascur, A unified solid/liquid separation framework, *Fluid/Particle Sep. J.* **4** (1991) 117–122.
4. N. Bellomo and C. Dogbe, On the modeling of traffic and crowds: A survey of models, speculations, and perspectives, *SIAM Review* **53** (2011) 409–463.
5. B. Boutin, C. Chalons and P.-A. Raviart, Existence result for the coupling problem of two scalar conservation laws with Riemann initial data, *Math. Models Methods Appl. Sci.* **20** (2010) 1859–1898.
6. C. E. Brennen, *Fundamentals of Multiphase Flow* (Cambridge University Press, 2005).
7. E. Brown and M. Shearer, A scalar conservation law for plume migration in carbon sequestration, *SIAM J. Appl. Math.* **78** (2018) 1823–1841.
8. R. Bürger, S. Diehl and M. C. Martí, A conservation law with multiply discontinuous flux modelling a flotation column, *Networks Heterog. Media* **13** (2018) 339–371.
9. R. Bürger, S. Diehl, M. C. Martí and Y. Vásquez, A numerical scheme for a triangular system of conservation laws with discontinuous flux modelling flotation with sedimentation, 2019, in preparation.

10. R. Bürger, A. García, K. H. Karlsen and J. D. Towers, A family of numerical schemes for kinematic flows with discontinuous flux, *J. Eng. Math.* **60** (2008) 387–425.
11. R. Bürger, A. García and M. Kunik, A generalized kinetic model of sedimentation of polydisperse suspensions with a continuous particle size distribution, *Math. Model. Meth. Appl. Sci.* **18** (2008) 1741–1785.
12. R. Bürger and K. H. Karlsen, On a diffusively corrected kinematic-wave traffic model with changing road surface conditions, *Math. Models Methods Appl. Sci.* **13** (2003) 1767–1799.
13. R. Bürger, K. H. Karlsen and J. D. Towers, A model of continuous sedimentation of flocculated suspensions in clarifier-thickener units, *SIAM J. Appl. Math.* **65** (2005) 882–940.
14. M. C. Bustos, F. Concha, R. Bürger and E. M. Tory, *Sedimentation and Thickening: Phenomenological Foundation and Mathematical Theory* (Kluwer Academic Publishers, Dordrecht, The Netherlands, 1999).
15. E. B. Cruz, A comprehensive dynamic model of the column flotation unit operation, Ph.D. thesis, Virginia Tech, Blacksburg, Virginia, 1997.
16. J. E. Dickinson and K. P. Galvin, Fluidized bed desliming in fine particle flotation – part I, *Chem. Eng. Sci.* **108** (2014) 283–298.
17. S. Diehl, On scalar conservation laws with point source and discontinuous flux function, *SIAM J. Math. Anal.* **26** (1995) 1425–1451.
18. S. Diehl, A conservation law with point source and discontinuous flux function modelling continuous sedimentation, *SIAM J. Appl. Math.* **56** (1996) 388–419.
19. S. Diehl, Operating charts for continuous sedimentation I: Control of steady states, *J. Eng. Math.* **41** (2001) 117–144.
20. S. Diehl, The solids-flux theory – confirmation and extension by using partial differential equations, *Water Res.* **42** (2008) 4976–4988.
21. S. Diehl, A uniqueness condition for nonlinear convection-diffusion equations with discontinuous coefficients, *J. Hyperbolic Differential Equations* **6** (2009) 127–159.
22. S. Diehl and S. Farås, A reduced-order ODE-PDE model for the activated sludge process in wastewater treatment: Classification and stability of steady states, *Math. Models Meth. Appl. Sci.* **23** (2013) 369–405.
23. G. A. Ekama, J. L. Barnard, F. W. Günthert, P. Krebs, J. A. McCorquodale, D. S. Parker and E. J. Wahlberg, *Secondary Settling Tanks: Theory, Modelling, Design and Operation* (IAWQ scientific and technical report no. 6. International Association on Water Quality, England, 1997).
24. G. A. Ekama and P. Marais, Assessing the applicability of the 1D flux theory to full-scale secondary settling tank design with a 2D hydrodynamic model, *Water Res.* **38** (2004) 495–506.
25. A. A. Eskin, G. A. Zakharov, N. S. Tkach and K. V. Tsygankova, Intensification dissolved air flotation treatment of oil-containing wastewater, *Modern Applied Sci.* **9** (2015) 114–124.
26. R. Etchepare, H. Oliveira, A. Azevedo and J. Rubio, Separation of emulsified crude oil in saline water by dissolved air flotation with micro and nanobubbles, *Sep. Purif. Tech.* **186** (2017) 326–332.
27. J. A. Finch and G. S. Dobby, *Column Flotation* (Pergamon Press, London, 1990).
28. K. P. Galvin and J. E. Dickinson, Fluidized bed desliming in fine particle flotation – part II: Flotation of a model feed, *Chem. Eng. Sci.* **108** (2014) 299–309.
29. K. P. Galvin, N. G. Harvey and J. E. Dickinson, Fluidized bed desliming in fine particle flotation – part III flotation of difficult to clean coal, *Minerals Eng.* **66-68** (2014) 94–101.

30. T. Gimse and N. H. Risebro, Riemann problems with a discontinuous flux function, in *Third International Conference on Hyperbolic Problems, Theory, Numerical Methods and Applications*, eds. B. Engquist and B. Gustavsson (1990), volume I, pp. 488–502.
31. S. K. Godunov, A finite difference method for the numerical computations of discontinuous solutions of the equations of fluid dynamics, *Mat. Sb.* **47** (1959) 271–306, (In Russian).
32. H. Holden and N. H. Risebro, *Front Tracking for Hyperbolic Conservation Laws* (Second Edition, Springer Verlag, Berlin, 2015).
33. K. H. Karlsen and J. D. Towers, Convergence of a Godunov scheme for conservation laws with a discontinuous flux lacking the crossing condition, *J. Hyperbolic Differential Equations* **14** (2017) 671–701.
34. S. N. Kružkov, First order quasilinear equations in several independent variables, *Math. USSR-Sb.* **10** (1970) 217–243.
35. G. J. Kynch, A theory of sedimentation, *Trans. Faraday Soc.* **48** (1952) 166–176.
36. E. J. La Motta, J. A. McCorquodale and J. A. Rojas, Using the kinetics of biological flocculation and the limiting flux theory for the preliminary design of activated sludge systems. I: Model development, *J. Environ. Eng.* **133** (2007) 104–110.
37. O. A. Oleinik, Uniqueness and stability of the generalized solution of the Cauchy problem for a quasi-linear equation, *Uspekhi Mat. Nauk* **14** (1959) 165–170, Amer. Math. Soc. Trans. Ser. 2, 33, (1964), pp. 285–290.
38. R. Pal and J. Masliyah, Flow characterization of a flotation column, *Can. J. Chem. Eng.* **67** (1989) 916–923.
39. J. F. Richardson and W. N. Zaki, Sedimentation and fluidization: part I., *Trans. Inst. Chem. Engineers (London)* **32** (1954) 35–53.
40. J. Rubio, M. L. Souza and R. W. Smith, Overview of flotation as a wastewater treatment technique, *Minerals Eng.* **15** (2002) 139–155.
41. J. Saththasivam, K. Loganathan and S. Sarp, An overview of oil–water separation using gas flotation systems, *Chemosphere* **144** (2016) 671–680.
42. P. Stevenson, S. Ata and G. M. Evans, Convective–dispersive gangue transport in flotation froth, *Chem. Eng. Sci.* **62** (2007) 5736–5744.
43. P. Stevenson, P. S. Fennell and K. P. Galvin, On the drift-flux analysis of flotation and foam fractionation processes, *Can. J. Chem. Eng.* **86** (2008) 635–642.
44. Y. Tian, M. Azhin, X. Luan, F. Liu and S. Dubljevic, Three-phases dynamic modelling of column flotation process, *IFAC-PapersOnLine* **51** (2018) 99–104.
45. J. D. Towers, Convergence of the Godunov scheme for a scalar conservation law with time and space discontinuities, *J. Hyperbolic Differential Equations* **15** (2018) 175–190.
46. J. Vandenberghe, J. Choung, Z. Xu and J. Masliyah, Drift flux modelling for a two-phase system in a flotation column, *Can. J. Chem. Eng.* **83** (2008) 169–176.
47. G. B. Wallis, *One-dimensional Two-phase Flow* (McGraw-Hill, New York, 1969), 281 pp.
48. G. B. Wallis, The terminal speed of single drops or bubbles in an infinite medium, *Int. J. Multiphase Flow* **1** (1974) 491–511.